JIMMA UNIVERSITY

JIMMA INSTITUTE OF TECHNOLOGY

SCHOOL OF POST- GRADUATE STUDIES

FACULTY OF CIVIL AND ENVIRONMENTAL ENGINEERING

HYDROLOGY AND HYDRAULIC ENGINEERING CHAIR

MASTER OF SCIENCE IN HYDRAULIC ENGINEERING

SPATIOTEMPORAL ANALYSIS OF FINCHA LAKE DYNAMICS USING GEOSPATIAL TECHNIQUES

BY

JABESSA BORU URGA

A THESIS SUBMITTED TO THE CHAIR OF HYDROLOGY AND HYDRAULIC ENGINEERING, JIMMA INSTITUTE OF TECHNOLOGY, JIMMA UNIVERSITY IN PARTIAL FULFILLMENT OF THE REQUIREMENTS FOR THE DEGREE OF MASTER OF SCIENCE IN HYDRAULIC ENGINEERING

JULY 1, 2024

JIMMA, ETHIOPIA

JIMMA UNIVERSITY

JIMMA INSTITUTE OF TECHNOLOGY

SCHOOL OF GRADUATE STUDIES

FACULTY OF CIVIL AND ENVIRONMENTAL ENGINEERING

HYDROLOGY AND HYDRAULIC ENGINEERING CHAIR

MASTERS OF SCIENCE IN HYDRAULIC ENGINEERING

SPATIOTEMPORAL ANALYSIS OF FINCHA LAKE DYNAMICS USING GEOSPATIAL TECHNIQUES

BY: JABESSA BORU URGA

A THESIS SUBMITTED TO THE CHAIR OF HYDROLOGY AND HYDRAULIC ENGINEERING, JIMMA INSTITUTE OF TECHNOLOGY, SCHOOL OF GRADUATE STUDIES, JIMMA UNIVERSITY IN PARTIAL FULFILLMENT OF THE REQUIREMENTS FOR THE DEGREE OF MASTER OF SCIENCE IN HYDRAULIC ENGINEERING

Main Advisor Dr. Ing.: Keneni Elias

Co-Adviser Natinael Sitota (MSc).

JULY 1, 2024

JIMMA, ETHIOPIA

DECLARATION

I, the undersigned, certify that this thesis, "Spatiotemporal Analysis of Fincha Lake Dynamics Using Geospatial Techniques." is my original work and has not been submitted for degree at Jimma University or any other university. I also certify that all sources of information used in the thesis have been properly cited and acknowledged.

Name Jabessa Boru

Signature ______________________________

Date ______________________________

To the best of our knowledge as supervisors, we hereby confirm that we have read and evaluated the thesis entitled "Spatiotemporal Analysis of Fincha Lake Dynamics Using Geospatial Techniques."

Dr. Ing.: Keneni Elias	-------------	-----------
Name of the main advisor	Signature	Date
Natinael Sitota (MSc).	-------------	------------
Name of Co-advisor	Signature	Date

APPROVAL

This thesis entitled with'' Spatiotemporal Analysis of Fincha Lake Dynamics Using Geospatial Techniques" has been approved by the following examiners for partial fulfilment of the requirement for the degree of Master of Science in Hydraulic Engineering.

Mr. JABESSA BORU URGA	----------------	------------
Candidate	Siganature	Date
Dr. Ing.: Keneni Elias	-----------------	------------
Name of the main advisor	Signature	Date
Natinael Sitota (MSc).	-------------	------------
Name of Co-advisor	Signature	Date

As members of the Board of Examiners of the MSc Thesis Open Defense Examination, we Certify that we have read, evaluated the Thesis prepared by Jabessa Boru and examined the candidate. We recommended that the Thesis be accepted as fulfilling the requirement for the degree of Master of Science in Hydraulic Engineering.

Members of Examining Board

Mr. Kasa Tadele (Dr)	-------------------	----------------
External Examiner	Signature	Date
Mr. Walabumma Oli (MSc)	---------------	----------------
Internal Examiner	Signature	Date
Nasir Gebi (Ass.Prof)	--------------	--------------
Name of Chairperson	Signature	Date

ACKNOWLEDGEMENT

Most importantly, I am grateful to my All-Powerful God, who has given me health and enabled me to overcome all obstacles in both my life and my studies. I am deeply appreciative to my adviser, Dr. Ing. Keneni Elias, and my co-advisor, Natinael Sitota (MSc), for their continuous advice and guidance from the start of proposal preparation until the end of the project. I want to sincerely thank them for all of their encouragement and moral support during the study period.

Lastly, I would like to express my gratitude to everyone who helped me to make my studies successful from the start to the finish, especially my dear family for their inspiration and encouragement, which sounds wonderful, and all of my friends for their suggestions and support. Last but not least, I would like to express my heartfelt appreciation to Mr. Gadefa Fikadu and Buli Tafara for their support

ABSTRACT

Lakes and reservoirs are vital for human health and aquatic life. In Ethiopia's Fincha sub-basin, water demand is rising rapidly, affecting Fincha Lake. Uncontrolled water abstraction, traditional watershed management practices, and land use changes may contribute to the Lake water level fluctuations. This study analyzes the changes in water area of Fincha Lake from 1990 to 2022 using remote sensing data from the Landsat platform. The objective of this study is to analyzed the spatiotemporal variations of Fincha Lake using geospatial techniques. Spectral water indices like the Automatic Water Extraction Index (AWEI), Water Ratio Index (WRI), Modified Normalized Difference Water Index (MNDWI), and Normalized Difference Water Index (NDWI) were applied to analysis lake waterbodies and area variations of Fincha lake. MNDWI and AWEI are the most effective, with MNDWI achieving 97.5% accuracy and a kappa coefficient of 0.93, and AWEI achieving 95% accuracy and a kappa coefficient of 0.92, respectively. Fincha Lake's surface area was measured in January of 1990, 2000, 2012, and 2022. In 1990, 182.13 km^2 were observed; in 2000, 190.08 km^2; in 2012, 173.98 km^2; and in 2022, 197.25 km^2. The lake's surface size increased dramatically by around 7.95 km^2 between 1990 and 2000. By 2012, though, it had decreased by about 16.1 km^2. The surface area increased significantly by around 23.27 km^2 in 2022. These measurements show that Fincha Lake's surface area fluctuated throughout the duration of the observation period, showing major increases in 2000 and 2022 as well as a notable decline in 2012. The study also examined land cover changes around the lake. To preserve Fincha Lake's ecohydrology, integrated watershed management and sustainable water resource management are essential. Satellite and remote sensing data address significant gaps in data-poor locations like Fincha Lake, supporting integrated water management and environmental conservation. This data facilitates the development of plans and informs stakeholders in order to improve decision-making.

Keywords: ***Geospatial techniques, Fincha Lake, Water Indices, water body extraction, Change Detection***

TABLE OF CONTENTS

Contents

LIST OF TABLES

LIST OF FIGURES

ACCRONYM

AWEI	Automated water extraction index
CRV	Central Rift Valley
DEM	Digital Elevation Model
ENVISAT	Environmental Satellite
ERDAS	Earth Resource Data Analysis System
ETM+	Enhanced Thematic Mapper Plus
GLAS	Geoscience Laser Altimeter System
GPS	Global Positioning System
ICESat	Ice, Cloud, and land Elevation Satellite
Kc	Kappa coefficient
LPGS	Level Product Generation System
ML	Maximum likehood
MIR	Mid-infrared band
MNDWI	Modified Normalized Difference Water Index
NASA	National Aeronautics and Space Administration
NDBI	Normalised Difference Built-up ndex
NDMI	Normalized Difference Moisture Index
NDVI	Normalized Difference Vegetation Index
NDWI	Normalized difference water index
OA	Overall accuracy
OLI	Operational Land Imager
RF	Random forest
SLC	Scan Line Corrector
SWIR	Short-Wave Infrared
TIN	Triangular Irregular Network
TIRS	Thermal Infra-Red Scanner sensors
TM	Thematic Mapper
TOPEX	Topology Ocean Experiment
USGS	United States Geological Survey
WRI	Water Ratio Index

1. INTRODUCTION

1.1. Background of the Study

The existence of aquatic species and human well-being depends on surface water bodies like reservoirs and lakes, even though they make up a small percentage of the earth's surface (Buma et al., 2018). Surface water bodies, including reservoirs, are dynamic because they shrink, expand, or change due to natural and human-induced phenomena (Karpatne et al., 2016). Lakes around the world are decreasing or drying up, as shown in studies by(Crétaux et al., 2016; and Pekel et al., 2016). However, the Lake Urmia in Iran has shown significant surface area shrinkage over 31 years (Jeihouni et al., 2017). The Deepor Beel lake in Guwahati, Assam, has shown a decrease in storage capacity over the last two decades (Ahmed et al., 2021). However, the Volta Lake in Ghana has shown an increase in surface water storage (Ghansah et al., 2016). In this regard, some Ethiopian lakes' surface area is changing dramatically either rising or falling.

For instance, according to Mengiste, (2019) the water level/area of Lake Abaya is rapidly increasing. On the other hand, Lakes Ziway, Langano, Shala, and Abijata have seen a considerable reduction in surface area and volume (Asfaw et al., 2020). Monitoring changes in lake water storage is critical for understanding the long-term impact of climate and land use change, as well as human activities on water availability (Lin et al., 2020; Treichler et al., 2019). Deforestation and land degradation caused by soil erosion, overgrazing, and inappropriate land use contribute to the shrinking of water bodies like reservoirs, wetlands, and lakes (Lemi, 2019). Studies have assessed factors affecting water availability, such as land use land cover, climate change, and catchment hydrology change in the Fincha sub-basin (Dibaba et al., 2020a, 2020b; Leta & Demissie, 2021).

Therefore, accurate monitoring and evaluation of lake water level variations are important for equitable water distribution among different users. Water levels, surface areas, and volume fluctuations are integrated to construct a time series indicating the lake's water storage variation (Asfaw et al., 2020). This suggests that lake shrinkage and expansion significantly affect agricultural water consumption, household water supply, hydropower energy production, and ecological activities. The lack of water level observations for ponds, lakes, and reservoirs worldwide has limited the quantification of reservoir changes in surface water storage compared to natural variability (Cooley et al., 2021). Previous studies have relied on ground-based reservoir/lake level recordings and altimetry-based data analysis (Chen & Duan, 2022).

Satellite-based remote sensing has numerous advantages for environmental monitoring, including land, water, air pollution, and lake level management (Wu et al., 2021b, 2021a). The extraction of water surface areas using remotely sensed data is commonly, used for reservoir/lake water level delineation (Nandi et al., 2018). Remote sensing and GIS are supplementary solutions for water resource management, providing cost and time-effective estimation of storage capacity, requiring minimal human supervision, and being reliable over long periods and in all weather conditions (Kushwaha et al., 2022). The agreement between measured and remotely sensed reservoir areas was satisfactory, demonstrating the usefulness of remotely sensed images for water management in Finchaa Lake. Multi-spectral indices and thresholding techniques are widely used to extract surface water bodies from optical remote sensing images due to their simplicity and speed (Sathianarayanan, 2018; Water et al., 2018; Yulianto et al., 2022). Several water spectral indices such as AWEI, NDWI, MNDWI, and WRI, have been developed for identifying surface water (Feyisa et al., 2014; Shen & Li, 2010; Xu, 2006, McFeeters, 1996). These indices have been used not only for vegetation identification but also for water extraction.

In this study, the changes of Finchaa Lake from 1990 to 2022 were studied using satellite-multiband water indexed methods. These methods include NDWI, MNDWI, WRI, and AWEI, using images from Landsat-5 TM, Landsat-7 ETM+, and Landsat-8 OLI for extracting the surface water body. The study used multi-sensor satellite remote sensing data to monitor the variation in water surface area of Finchaa Lake. The objective of the study is to analyze the changes in available water surface area within the Fincha reservoir/lake from 1990 to 2022 using satellite imagery from Landsat platforms.

1.2. Statement of the problem`

Despite the fact that various investigations have been conducted to analyze lake level changes by researchers around the globe, there is still a limited scientific assessment of lake surface level, area, and volume in the context of Ethiopian lakes. Numerous studies have examined lake/reservoir area and water level changes using observations from lake hydrological stations (Goshime et al., 2019; Shift et al., 2021), and, to some extent, satellite remote sensing imagery (Hailu & Girma, 2019; Shumet & Mengistu, 2016). Additionally, in recent times, water availability in reservoirs/lakes in the Upper Blue Nile Basin, particularly in the Fincha sub-basin, has become a critical problem due to water resource scarcity (Mohammed, 2020). For instance, a study conducted by Leta et al., (2021) found that the Fincha sub-basin is experiencing intensive conversion of forest and virgin land into agricultural activities, leading to overgrazing and deforestation.

Consequently, this has caused a reduction in the capacity of the Fincha reservoir due to sedimentation, as outlined by the author. However, the authors did not discuss the impacts of these environmental changes on reservoir water surface change and the lakes micro-hydrologic cycle, nor did they discuss the spatial scales at which these changes occur. Moreover, the reason behind selecting this study area is that Fincha Lake is one of the most extensively utilized artificial lakes in the Fincha sub-basin of Ethiopia. To address this data gap, a simple method for estimating surface area based on LANDSAT remotely sensed lake surface area was developed. To the best of the author's knowledge, no previous study has carefully examined the Fincha Lake water level changes. Hence, the extent of such variation is not well-documented using a geospatial approach. Consequently, this research was carried out to analyze the spatiotemporal variations of Fincha Lake water area for the period ranging from 1990 to 2022 using remote sensing data from multiple satellite datasets.

1.3. Objectives of The Study

1.3.1. General Objective

This research paper aims to conduct a spatiotemporal analysis of Fincha Lake dynamics using geospatial techniques.

1.3.2. Specific Objectives

- To identify the best-performing indices for surface water portion detection using multi-temporal Landsat data.
- To evaluate Spatiotemporal Variations of Fincha Lake's Surface Water Area Using Remote Sensing Indices (1990-2022)
- To assess land use and land cover change detection using remote sensing in the Lake Fincha

1.4. Research Questions

The research questions of the present study were:

- What are the most effective spectral indices for detecting surface water bodies using multi-temporal Landsat data, and how do their performances compare?
- What are the magnitudes of variations in Fincha Lake surface area for the years 1990, 2000, 2012, and 2022?

- What is the impact of land use and land cover on the extent of lake Finchaa and its surroundings?

1.5. Significance of the study

The study basic input for future water use scheme planning, implementation, and monitoring, as well as further optimal use to fulfil the increasing demands for basic human requirements and wellbeing. This research might be useful to policymakers in developing sustainable agriculture, hydropower and industrial water usage strategies to save water resources and prepare systems of reservoir operation and governance policies under changing environment. To this end, it is envisaged that this lake water level variations evaluation bringings very useful means to adjust water resource management strategies, mainstreaming reservoir management principles under competing factors and environmentalists to considering climate change repercussion on the surface water availability of Fincha Lake. In addition, it will give insights to intervention means and also used as benchmarking for further research works.

1.6. Scope of the study

Geographically, the study is limited to Fincha Lake, which is located in the Fincha sub-basin in the Horro Guduru Wollega Zone in western part of Ethiopia. Methodologically, the study is also limited to Spatiotemporal Analysis of Fincha Lake Dynamics Using Geospatial Techniques for the period of 1990 to 2022 using remote sensing data from multiple satellite datasets. In this study Landsat satellite imagery is selected for mapping surface area of the lake. The image is selected because of its freely availability and appreciable spatiotemporal and spectral resolution.

2. LITERATURE REVIEW

2.1. Lakes water area fluctuations and their trends in Ethiopia

The underlying causes for the lake water level fluctuations to be occurred are multifarious that include both natural and anthropogenic factors(Minale, 2020a). According to Ye et al.,(2017), declining of water levels of lakes and reservoirs will produce a series of environmental problems, such as wetland area shrinkage of wetland area, species diversity reduction, water quality deterioration, and fish production reduction, etc. For example, Lake Tana area, like that of many other lakes around the world, has been changing as a result of anthropogenic activities(Minale, 2020b). According to (Bulti & Minch, 2019) indicated average water body areas all showed a typical decreasing trend from 2009 to 2018, but the year-long water area showed a slight upward trend. Recently, (Sisay, 2016) report abrupt change of Lake Abiyata (-68 km 2) over the past four decades and unappreciable changes of Lake Shala and Langano using six multi-temporal Landsat imageries with the help of two water surface extraction indices. For instance, study done by (Sisay, 2016) show that Lake Shala and Lake Langano has shown very small changes (-3.68 sqkm & -10.2 sqkms respectively) as compared to the surface area change of Lake Abjata (-68 sqkm) between 1973 and 2014, hence making Lake Abjata the most abruptly changing lake in four decades. Except for a small number of lakes affected by human activity, most of the rift lakes fluctuate in response to the local climate (Diress & Besha Bedada, 2020) Changes in the rainfall conditions over the nearby highlands are also reflected in the recent variations in lake level. For the past 40 years, there hasn't been a downward trend in rainfall in the area, other from interannual and seasonal fluctuations.

2.2. Geospatial techniques for Monitoring water bodies

Environmental policymakers can better understand surface water supplies by using water body extraction. In order to monitor changes in surface water, remote sensing technology plays a critical role by providing fast and accurate surface water information extraction (Region, 2020). Various algorithms have been implemented for studying changes in water bodies, particularly using Landsat data that can be divided into four primary categories: First, there are supervised (Sathianarayanan, 2018) and unsupervised (Y. Zhang et al., 2018) approaches for pattern recognition and classification. Second, Experimental et al., (2023) describe spectral un-mixing. Third, the spectral water index (Ruimeng Wang et al., 2021), and fourth, the single band threshold (Sisay, 2016). Further, Naik & Anuradha, (2020) was analyzes waterbodies using unsupervised classification, supervised classification, single-band threshold, inter spectrum relation method, and water index method (normalized difference water index, modified normalized difference water index, and new water index). For further information on identifying, extracting, and tracking surface water by optical remote sensing, see the recent review of spectral water index by (Acharya et al., 2018). In final analysis, the use of remote sensing methods for extracting water bodies offers an effective instrument for managing and monitoring the environment. Through the utilisation of spectral indices, thresholding techniques, and classification methods, researchers may efficiently monitor surface water changes, hence aiding in the creation of sustainable policies and management practices.

2.2.1. Extraction of Surface Water by Single-Band Threshold Method

The single-band threshold method provides a simple and computationally efficient approach for extracting surface water from remote sensing imagery, making it suitable for large-scale water mapping applications(Ji et al., 2019). By using the proper threshold, the single-band threshold approach extracts the information about the water body by first identifying a particular band in the remote sensing image where the difference between the water body and other background characteristics is the greatest(Sun & Li, 2024). The thresholding method establishes a threshold for a single band or many bands based on the spectral differences between water and other ground objects, and then determines which items are water and which are not. Additionally, a number of studies have created more efficient surface water extraction techniques by utilizing water index approaches. Ali et al., (2019) uses spectral relation, single-band threshold, and shade water body index (SWI) methodologies as the primary techniques for extracting information about water bodies from remote sensing data. However, research by Region, (2020) compared different water body extraction methods based on satellite data and extracted Poyang Lake's surface water using the single-band threshold method and the water index method. By using a suitable threshold, the single-band threshold approach extracts the information about the water body by first identifying a particular band in the remote sensing image where the difference between the water body and other background characteristics is the greatest (Sathianarayanan, 2018).

2.2.2. Extraction of Surface Water by Water Index Method

Spectral indices that are specifically created to identify, water features in remote sensing data must be calculated in order to extract surface water using the water index approach. By utilizing the spectral characteristics of water and accounting for variations in environmental conditions, the water index method provides a more advanced method of extracting surface water than single-band thresholding(Sathianarayanan, 2018). However, in order to ensure accurate results, it requires careful selection of spectral bands, computations of indices, and validation. Use mathematical combinations of reflectance values from the selected spectral bands, to calculate water indices. The Automated Water Extraction Index (AWEI), Modified Normalized Difference Water Index (MNDWI), and Normalized Difference Water Index (NDWI) are a few examples of commonly used water indices. On the other hand, a study, conducted by (Eghod and Egho, (2016) aimed to extract the surface water area from Landsat images using different techniques, including WRI, NDVI, NDWI, MNDWI, AWEI, and NDMI. In this study, satellite images were derived using MNDWI, NWDI, WRI, and AWEI as the indices used to extract lake water bodies from TM, ETM^+, and OLI images. Deoli et al., (2022) used QGIS software, and the spectral index approach served as the basis for NDWI, MNDWI, and WRI. One popular water index is the Normalized Difference Water Index (NDWI)(McFeeters, 2007) .The Modified Normalized diference Water Index was developed to overcome the problem of water pixels mixed with built-up features (Xu, 2019). The Automated Water Extraction Index (AWEI) was introduced to achieve better results when the Landsat image contains shadow and dark surfaces. The Water Ratio Index (WRI) is another widely used water index according to Sathianarayanan, (2018). The spatial as well as temporal changes in the volume of water bodies can be calculated by several methods depending on the availability of morphometric and areal data. Lake area, water level, and volume are critical indicators in the study and management of lake hhydrology and water availability in reservoirs.

2.2.3. Surface Water Extraction Using Supervised and Unsupervised Classification Technique

Algorithms are used to automatically categorize pixels in remote sensing pictures into classes related to water and non-water in order to extract surface water using supervised and unsupervised classification techniques. These techniques classify pixels in the entire image by first using training data to identify the spectral properties of water and non-water objects (Abbas & Jaber, 2020). Automated techniques for extracting surface water from remote sensing pictures are provided by both supervised and unsupervised classification algorithms(Naik & Anuradha, 2020). Unsupervised classification finds spectral classes on its own without the requirement for predefined training samples, whereas supervised classification needs training data but gives the user more control over the classification procedure (Abbas & Jaber, 2020). A research conducted by Naik & Anuradha (2020) using supervised and unsupervised classification algorithms assessed the dynamic changes in the spread surface water area in the

Nagarjuna Sagar reservoir from 2014 to 2019. Undoubtedly, supervised classification methods exhibit exceptional accuracy in extracting water extent by leveraging the spectral, shape, and other relevant features through training processes with extensive water body samples.

2.3. Spectral indices for water body detection

Analysing the efficacy of water indices in monitoring ecosystem health, quantity, and quality is part of evaluating their performance. Choosing relevant indices, gathering information, implementing the indices, and analysing the outcomes are usually the steps in the technique for such an assessment. Numerous water indices, such as NDWI Mcfeeters, (2007), MNDWI Xu, (2006), AWEI Fisher et al., (2016), and WRI F. Zhang et al., (2011), have been employed in the analysis of Landsat imagery. Sisay, (2016), for instance, used Landsat data to determine how three lakes in Ethiopia's south have changed in size over time. Fisher et al., (2016a) reported that WRI and AWEIsh performed best, whereas NDWI, MNDW, and AWEInsh performed least accurately. Both quantitative accuracy indicators of overall correctness, producer accuracy, and user accuracy were used to assess the indices in addition to qualitative visual examination. In the research region, a comparative evaluation of little water extraction methods (NDWI, MNDWI, NDMI, AWEIsh, and WRI) is carried out Khalid et al., (2021). In a Landsat 8 scene of Nepal, the study Acharya et al., (2018) assessed the performance of the most popular water indices, including the Automated Water Extraction Index (AWEI), Modified NDWI (MNDWI), Normalized Difference Water Index (NDWI), and Normalized Difference Vegetation Index (NDVI). Feyisa et al., (2014)developed an automatic water extraction index (AWEI), using band addition, band differentiation, and the application of several coefficients to maximize the accuracy of classifying water pixels and non-water pixels. The most accurate methods for extracting surface water, according to the results, are the water index (WI) and the automatic water extraction index with shadow (AWEIsh) (Tesfaye & Breuer, 2023). Researchers found that Asfaw et al., (2020), showed that accuracy tests showed that the MNDWI and AWEI indices performed well while the NDW index did not perform as well.

2.4. Impact of the Threshold Value on the Performance of Water Mapping

Research conducted by Du et al., (2019.) NDWI is more sensitive to the change of the water mapping threshold value than MDNWI. If the threshold value of NDWI is larger than 0.1, the Kappa values of the resultant water maps will have a severe decrease. In general, the threshold is a fixed value, but it can be challenging in the case of environmental noise, such as shadow, forest, built-up areas, snow, and clouds Acharya et al., (2018). According to study Yulianto et al., (2022) show that, the accuracy of automatic lake surface water classification using an AWEI based on analysis and calculations, to determine the threshold value in classifying water and nonwater classes, and to conduct a test case study of AWEI threshold improvement results on the surface water of several lakes with a variety of different or heterogeneous characteristics. MNDWI and AWEI were unable to reject snow cover and shadows, whereas NDVI and NDWI performed better for only pure water pixels Acharya et al., (2016). Similarly, All water indices (including NDWI, AWEI, and even MNDWI) have inherent defects, such as classification errors caused by ice and snow, cloud shadows, topographic shadows, and building shadows (F. Zhang et al., 2018).

The effectiveness and accuracy of water indices for mapping water bodies from remotely sensed imagery can vary significantly based on the chosen threshold values and the environmental conditions present in the study area. Here's a detailed discussion on the findings from various studies regarding these water indices:

Sensitivity to Threshold Values:

Du et al., (2019.)found that the Normalized Difference Water Index (NDWI) is highly sensitive to changes in the threshold value used for classifying water and non-water areas. If the threshold value exceeds 0.1, the accuracy of the water maps, as indicated by the Kappa statistic, drops significantly. This sensitivity poses a challenge for consistent water body delineation, especially in heterogeneous environments.

Environmental Noise Impact:

Environmental noise such as shadows, forests, built-up areas, snow, and clouds complicates the application of fixed threshold values. Acharya et al., (2018) highlighted that these factors can introduce errors in water classification. Shadows from clouds, topography, and buildings can be mistaken for water, leading to misclassification. The studies underscore the challenges of applying fixed threshold values for water body classification across diverse environments. To address these challenges, researchers need to: Adjust threshold values based on specific environmental conditions and the characteristics of the study area. Utilize multi-temporal and multi-spectral data to improve classification robustness and reduce the impact of transient noise factors. Integrate ancillary data, such as elevation and land cover maps, to refine water body delineation and reduce misclassification. In summary, while water indices like NDWI, MNDWI, and AWEI are valuable tools for water body extraction from satellite imagery, their effectiveness is influenced by the chosen threshold values and environmental noise.

2.5. Effect of landcover/land-use changes on water availability

Research conducted in Ethiopia revealed that streamflow and hydrological cycle processes in several basins, sub-basins, and catchments were impacted by LULC change (Dibaba et al., 2020a) The study area has different LULC classes: cultivated land, forest, grassland, shrubs land, and settlements. In the research region, agricultural land is the most common kind of LULC (Moisa et al., 2023). A research conducted by Hailu & Girma, (2019 and Kenea et al., (2021) Both biophysical and anthropogenic driving variables cause the spatiotemporal pattern of LULC variations in different regions of Ethiopia. Changes in land use and cover have had a detrimental effect on the drainage basin system of the lake, which has led to Lake(Ali et al., 2019a). On the other hand, a research conducted by Regasa & Nones, (2022a) Land Use Land Cover Changes (LULC) in the Fincha River Basin of Ethiopia are primarily responsible for bare land growth, increased surface runoff generation, and soil erosion. The maximum likelihood algorithm of Landsat images supervised classification yielded the following four LULC categories, which were identified in the study region: urban areas (including residential, commercial, industrial, and road constructions); cultivated lands (including old cultivated lands and newly reclaimed lands); deserts (including bare lands, sand sheets, and rocky land); and water bodies (including the Nile River, canals, drainage patterns, and wastewater treatment plants)(Regasa & Nones, 2022a).

Overall, land cover and land-use changes can have complex and interconnected effects on water availability, impacting hydrological processes, water quality, and groundwater resources. Sustainable land management practices and integrated water resource management strategies are essential for mitigating adverse impacts and ensuring water security in the face of changing land use and climate conditions.

2.5.1. Integration of LULC and Water Indices in Studies

Land Use and Land Cover (LULC) data and water indices serve distinct purposes in remote sensing and hydrological studies. LULC data categorize the Earth's surface into different land cover types, such as forests, agriculture, urban areas, and water bodies, providing insights into landscape patterns and human-environment interactions. Future studies should investigate the hydrological response of sub-catchments to LULC changes and climatic variations. This includes understanding how land cover changes, such as deforestation or urbanization, impact water flow, sediment transport, and flood risks. Ali et al., (2019a) emphasized the importance of examining hydrological responses to both LULC changes and climatic influences to predict future water availability and ecosystem health. Investigate how LULC types correlate with various indices, such as the Normalized Difference Vegetation Index (NDVI), Normalized Difference Water Index (NDWI), and Normalized Difference Built-Up Index (NDBI). For example, Muralitharan et al., (2021)explored the relationship between land surface temperature (LST), LULC, and these indices in the Greater Arba Minch, Rift Valley, Ethiopia. Their study found significant associations between LST and indices like NDVI and NDWI, which vary across different LULC types and seasons. Additional Studies, M et al., (2020); and Muralitharan et al., (2021) highlighted the usefulness of remote sensing images for monitoring indices like NDVI, NDWI, and NDBI, providing timely and synoptic views of land cover changes. On the other hand, water indices are mathematical algorithms applied to multispectral imagery to identify and delineate water bodies based on their unique spectral signatures.

Future studies should look into the sub-catchment's hydrological response to potential climatic, variable, and changing influences as well as LULC changes(Ali et al., 2019a).Muralitharan et al., (2021) to extract the LST and examine its association in the greater Arba Minch, Rift valley, Ethiopia, with land-use/land-cover and the normalised difference vegetation index (NDVI), normalised difference water index (NDWI), and normalised difference built-up index (NDBI). By providing timely and synoptic views of land-based coverage, remote sensing images more suitable for monitor NDVI, NDWI, and NDBI (M et al., 2020; Muralitharan et al., 2021).Furthermore, LST has connections with NDVI, and NDWI, and it varies significantly in different LULC types and times (Huang et al., 2018) Water indices concentrate particularly on identifying and characterising water bodies, whereas LULC data offer information on more general land cover types and human activities. When combined, they provide supplementary understandings of environmental dynamics that help a range of applications in hydrological modelling, land use planning, and natural resource management.

3. MATERIALS AND METHODS

3.1. Description of The Study Area

The Fincha Lake is located in the Upper Blue Nile Basin in Ethiopia's Oromia regional state, Horo Guduru Wallega. This basin is located around 300 kilometres from Addis Ababa, between latitudes 9°20′0″ N and 9°40′0″ N and longitudes 37°10′0″ E and 37°30′0″ E. Figure 3.1 displays the detailed description of the study region. According to Regasa & Nones,(2022) there are four distinct seasons in this area: summer, with copious amounts of rainfall from June to August; autumn, which lasts from September to November and is known as the harvest season because of the excellent climate; Winter, particularly in January, is extremely dry from December to February and features morning frost. Spring, the hottest season with sporadic showers, lasts from March to May. The yearly rainfall ranges from 1367 to 1842 mm, with the Northern lowlands receiving the least amount of rain and the Southern and Western highlands receiving the most, exceeding 1500 mm. With an average of 1604 mm, June through September is the primary rainy season; July and August see the highest amounts. Large-scale sugar cane fields are irrigated by natural resources including the Fincha, Amarti, and Nashee lakes, which also serve as hydroelectric reservoirs and play a crucial role in meeting the region's energy needs. From a hydro-political perspective, this study region is crucial on a national and worldwide scale since it connects to the Nile basin and supplies water for intensive agriculture.

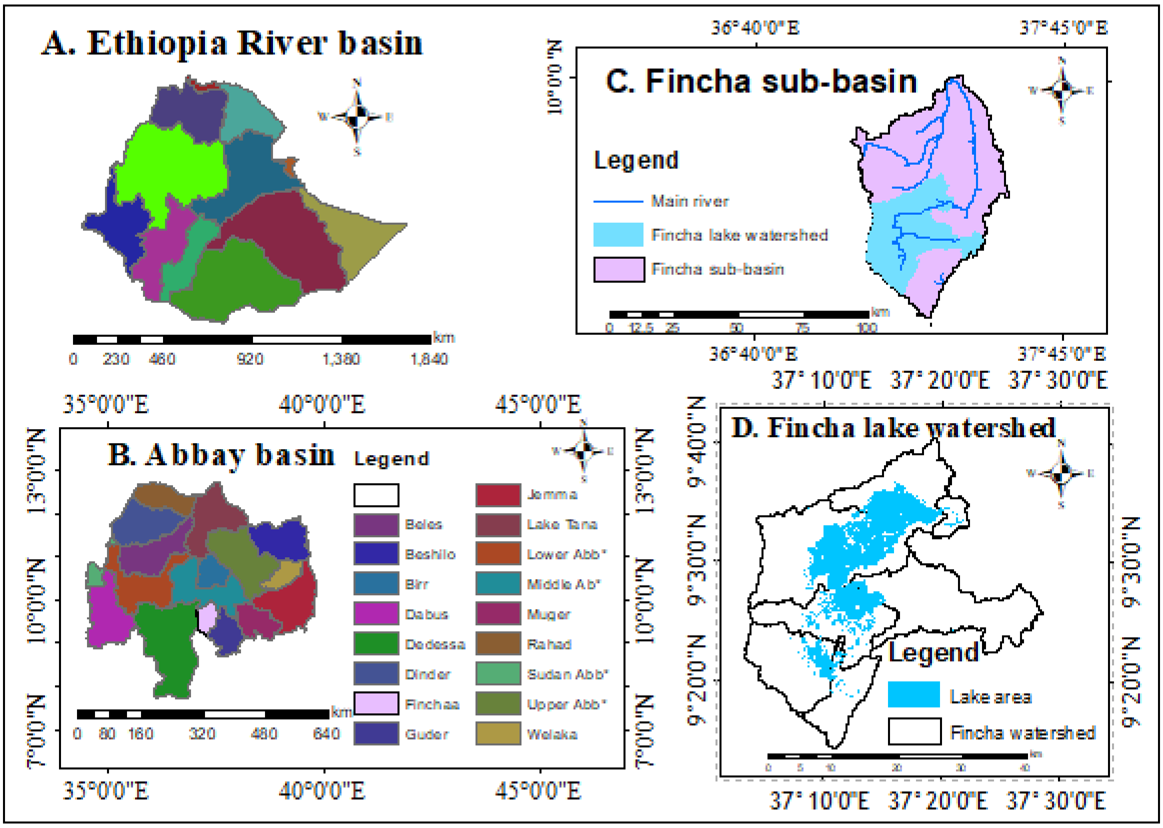

Figure 3-1 Location of study Area,

Large upstream water potential locations, heavily irrigated downstream fields, and significant hydropower potential are all present in the region. Fincha, Amerti, and Neshe are the three watersheds that make up the sub-basin (Kenea et al., 2021). The catchment's average monthly temperature ranges from 15.50 °C to 18.62 °C. Agroecologically, the Finchaa sub-basin is made up of hot to warm, humid lowlands in the northeast, wet mid-highlands in the southeast, and tepid to cold, sub-humid mid-highlands in the northwest of the catchment (Dibaba et al., 2020). The Fincha'a watershed has a temperate, humid climate because to its high elevation. The average annual rainfall from 1970 to 2003 was 1823 mm. Eighty percent of the rainy season occurs from May to September. Quaternary volcanic rock makes up the higher regions close to the watershed's edge as well as the elevated, solitary outcrops in the centre of the watershed. The watershed's predominant soils range in texture from clay to loam and clay-loam.

3.2. Remotely sensed data

The Landsat-5 TM, Landsat 7 ETM+, and Landsat-8 OLI data obtained the same season in January, 1990, 2000, 2012, and 2022. These data were taken from United States Geological Survey (USGS) provides L1TP data in GeoTIFF format individually for each band in WGS84

UTM (zone 37N) coordinate system. Table 3.1 and 3.2 presents further information on the Landsat spectral bands and geographical resolution. By employing these geospatial techniques and methodologies, analysts can gain valuable insights into Fincha Lake dynamics, contributing to effective environmental management and conservation efforts tailored to the lake's specific challenges and needs.

Table 3-1 Specifications of Landsat TM, ETM+ and OLI data.

Satellite	Date of Acquision	Path/Row	Spatial Resolution
Landsat 5 TM	07/01/1990	169/54	30*30
Landsat 7 ETM+	27/01/2000 and 12/01/2012	169/54 and 53	30*30
Landsat 8 OLI	31/01/2022	169/53	30*30

Table 3.1 shows the comparison of Landsat-5 TM, Landsat 7 ETM+, and Landsat-8 OLI. The water body was extracted from satellite images with a spatial resolution of 30m and different wavelength bands, as shown in

Table 3-2 Information of the Landsat spectral bands used in this study.

Band	Spectra Range			Resolution(m)
	TM	ETM+	OLI	
	Wavelength (μm)			
Blue	0.45 – 0.52	0.45 – 0.52	0.45 - 0.52	30
Green	0.52 – 0.60	0.52 – 0.60	0.53 – 0.60	30
Red	0.62 – 0.69	0.63 – 0.69	0.63 – 0.68	30
NIR	0.76 – 0.90	0.78 – 0.90	0.85 – 0.89	30
SWIR1	1.55 – 1.75	1.55 – 1.75	1.56 – 1.67	30
SWIR2	2.08 – 2.35	2.09 – 2.35	2.10 – 2.29	30

The water body was extracted from satellite images with a spatial resolution of 30m and different wavelength bands. Although this satellite has a low spatial resolution, it has a higher spectral resolution than is obtained by other satellites. Due to the scarcity of time series water surface and water level data for Finchaa Lake, the assessment of water resources is entirely dependent on the use of remotely sensed imagery. The investigation obtained digital elevation model (DEM) data for this study with a spatial resolution of 12.5 m × 12.5 m. The data was downloaded from the Alaska Satellite Facility website. Additionally, the Ethiopian Ministry of Water and Energy Office provided a topographic map of the research area. The topographic maps were used to analysed the drainage system/pattern, basin area, and sub-watershed boundaries of the research area. The DEM data was also utilized to compute flow direction and accumulation, analysed the stream networks derived from the DEM, and select the area to designate the sub-watershed after filling. With the use of this data, one may more effectively create variations to the lake measurements and gain a better understanding of the surface areas of the lake that are subject to watersheds for LULC objectives. In the final analysis, the study's utilisation of Landsat satellite imagery has many benefits, such as the ability to monitor for an extended period of time, data consistency, multisensory synergy, worldwide coverage, data accessibility, policy-making assistance, and ease of doing scientific research. This emphasises how important Landsat data is to expanding our understanding of the dynamic and interrelated systems that make up Earth. The study of Fincha Lake's dynamics using geospatial techniques involves acquiring and pre-processing satellite images, using classification methods, and analyzing spatial data. Change detection techniques include image differing, classification algorithms, and vegetation indices. GIS analysis measures lake area, shoreline changes, and areas susceptible to erosion or sedimentation. Modeling and prediction involve regression models and machine learning algorithms. Visualization and interpretation are done using GIS tools and interactive platforms. Reporting and decision support systems are prepared to inform decision-making. Validation and accuracy assessment involve ground truthing and error analysis. These techniques provide valuable insights into Fincha Lake's dynamics, aiding in effective environmental management and conservation efforts.

3.3. Land use land cover data collection and analysis

The Finchaa Lake land use and land cover types were classified using the analysis of Landsat image LULC types TM from 1990, ETM+ from 2000 and 2012, and OLI from 2022. For the supervised LULC classification, the maximum likelihood approach was used. ERDAS IMAGINE was used for the supervised image classification in order to produce the land use land cover map for the research area. Maximum Likelihood Supervised Classification is a powerful and effective method for analyzing the spatiotemporal variation of Fincha Lake. Its accuracy, ability to handle mixed pixels, consistent temporal application, integration with multispectral data, and adaptability to different environmental conditions make it a preferred choice for this type of analysis (Rui Wang et al., 2023). By leveraging MLSC, researchers can obtain detailed and reliable insights into the changes in Fincha Lake's surface area over time, contributing to better understanding and management of the lake's dynamics.

Four multitemporal remotely sensed images (Landsat TM 1990, Landsat ETM+ 2000 and 2012, and Landsat OLI 2022) were gathered for this study in order to detect changes. These pictures were downloaded as zipped files, which were then opened as Tiff format files. The satellite images used in this investigation were taken during the dry season. Dry seasons were selected because the clear, high-quality satellite images made it easy to discern between grazing and agriculture areas. LULC was identified from the satellite pictures using image processing and classification. LULC classes were developed using data from previously acquired knowledge, field observations of the sample sites, and ground control points. This structured approach, utilizing ERDAS Imagine for image processing and classification, along with a rigorous validation process, provides a comprehensive methodology for analysing land use and land cover changes in the Finchaa Lake area. The use of multitemporal Landsat images and the focus on the dry season enhance the clarity and accuracy of the LULC maps produced, supporting effective environmental and land management decisions.

3.4. Software packages

The study used various software packages, including ERDAS Imagine 2015, ArcGIS 10.4.3, and Arc SWAT tools. For instance, ERDAS Imagine 2015 was used for processing and classifying satellite images. This software is well-known for its strong remote sensing capabilities and tools for raster data processing, image analysis, and GIS data integration. Similarly, ArcGIS 10.4.1 was employed for detailed spatial data analysis and interpretation. It offers powerful mapping, spatial analysis, and data management tools for thorough geospatial investigations and decision-making (Babekir & Osman, 2024). Additionally, Arc SWAT (Soil and Water Assessment Tool) integrated with ArcGIS was utilized for hydrological modelling. It specifically helped extract drainage networks and delineate sub-basins. ArcGIS worked alongside Arc SWAT by facilitating spatial analysis and visualization to better understand watershed characteristics and hydrological processes (Modeling et al., 2023). Each software tool was chosen based on its ability to effectively manage specific aspects of the overall workflow, resulting in precise and comprehensive outcomes.

3.5. Remote sensing Data Analysis Techniques

3.5.1. Image pre-processing

Maximum likelihood techniques in Earth Resource Data Analysis System (ERDAS) imagine 2015 was used for Landsat image processing and classification. Images acquired by Landsat sensors are distorted due to sensor, solar, atmospheric, and topographic effects. Pre-processing tries to reduce these effects to the extent desired for a specific application (Young et al., 2017). To overcome issues caused by low-quality images, pre-processing is typically performed before extracting features from the image. The image was subjected to composite, mosaic, subsetting, and SLC correction during this process. In general, pre-processing steps such as composite, mosaic, subsetting, and SLC correction are essential for preparing satellite imagery for accurate and meaningful analysis. These steps help to address distortions and inconsistencies in raw imagery, ensuring that the data is suitable for a wide range of applications, including land use and land cover classification, change detection, and environmental monitoring.

3.5.2. Fixing scan line error

The failure of Landsat 7 Scan Line Corrector (SLC) imposed systematic data gaps on retrieved imagery and eliminated the ability to provide spatially continuous fields. On January 01, 2012 the scan line corrector (SLC) failed during download, and a data gap was discovered in ETM+ image therefore, for the SLC failure image, the simple gap-filling expansion toolbox in ERDAS is used to fill in the blank (Li et al., 2022). Scientists have devised methods to replenish absent information and reinstate the spatial coherence of the images. By guaranteeing precise depiction of spatial patterns and relationships, this approach facilitates trustworthy analysis and interpretation. In addition, gap-filling strategies support the continuity of long-term datasets, which is crucial for managing natural resources, urban planning, disaster relief, and environmental monitoring.

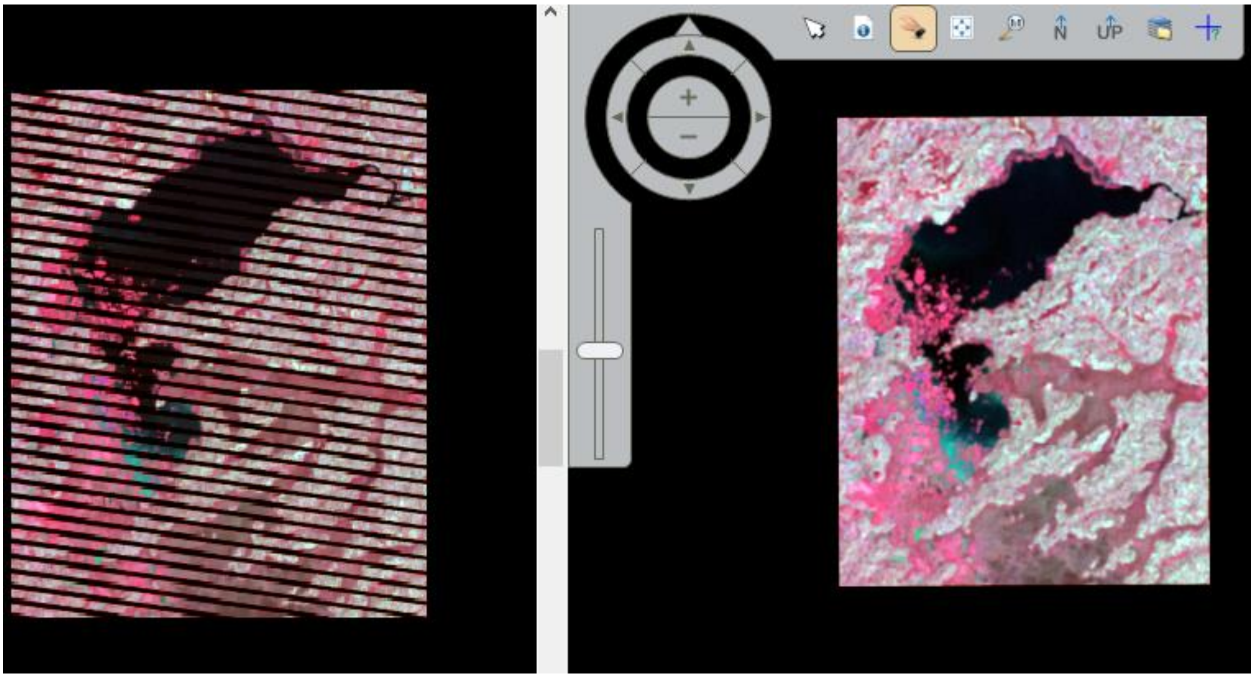

Figure 3-2 Before and after SLC-off Landsat 7 image gap filling

3.5.3. Image Layer stack

Layer stacking is the process of combining lots of individual bands to create a new multiband image. These multiband images are useful for visualizing and identifying the various Land Use

Land Cover classes. Multiple image bands must have the same extent in order to layer-stack (no. of rows and columns) Layer stack is the second step of image pre-processing. It is the process of adding multiple bands of an image and making a single layer. Typically, satellite images are delivered in a zipped folder containing multiple bands, such as 7,9 - or 11. To save processing time, stack only the bands that are required. Layer stacking is an essential technique for creating coherent multiband pictures from several spectral bands, which is useful in remote sensing applications. For many other types of analysis tasks, such as feature extraction, classification, and visualisation, these photos provide the basis for datasets. Layer stacking aids in the making of well-informed decisions in a variety of domains, including agriculture, urban planning, natural resource management, and environmental monitoring, by providing thorough analysis of Earth's surface features.

3.5.4. Mosaicking of an image

A mosaic is any two or more images combined, and "mosaicking" refers to the process of making a composite image. Since the current study covers large area, eight satellite images were mosaicked. Generally, ERDAS software was used for mosaicking of image for the study area. When working with enormous geographic areas that cannot be represented in a single camera frame, mosaicking is an essential technique in remote sensing and GIS applications. Mosaicking plays a crucial role in producing a thorough and cohesive picture of the entire research region in the context of this large-scale investigation. Here is a thorough explanation of the role that mosaicking plays in the study and its significance:

3.5.5. Subset

The process of reducing the size of an image by cutting the area of interest in a new image file is known as subset. It is the process of clipping area of interest using different tools. For current study subset of an image was done using ERDAS software. In the current study, subset processing—made possible by programmes like ERDAS software is essential to honing and concentrating picture analysis efforts. Subset processing improves the accuracy, speed, and efficacy of analytic workflows by separating out particular regions of interest from the broader picture collection. In the end, this method allows researchers to derive significant insights and arrive at well-informed conclusions through focused examination of pertinent areas within the research domain.

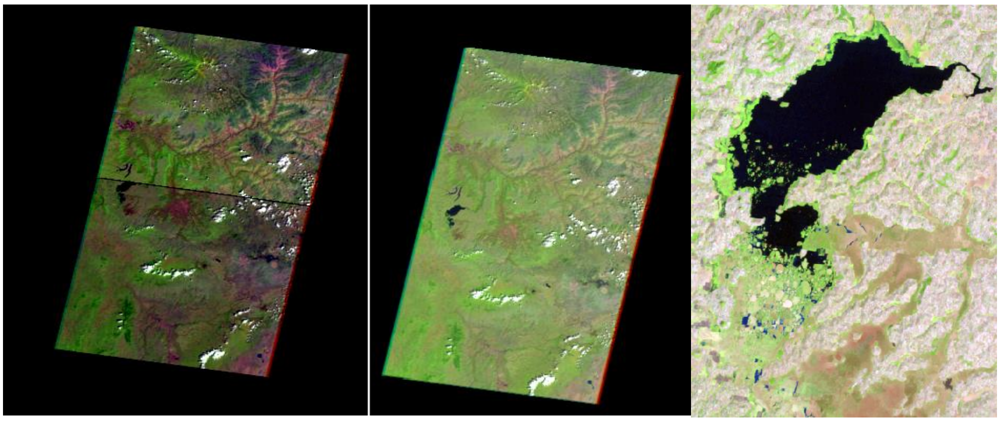

Figure 3-3 Finchaa Lake layer stacking, mosaic image and subsetted image

3.6. Spectral Index-Based Algorithms for Surface Water Extraction

Water bodies can be extracted from remotely sensed imagery using spectral water indexes, which are typically created by calculating the normalised difference between two picture bands and then classifying the findings into two groups (water and non-water features) using a suitable threshold. This work extracts lake water bodies from TM, ETM+, and OLI pictures using NDWI, MNDWI, WRI, and AWEI (Khalid et al., 2021; Sathianarayanan, 2018; and Yulianto et al., 2022). MNDWI, NDWI, WRI, and AWEI are more suitable for water body detection and monitoring due to their ability to effectively differentiate water from other land cover types, their applicability in various environments, and their facilitation of automated and accurate water extraction processes in remote sensing applications. Water body extraction from remotely sensed imaging is an important task in land use planning, hydrology, and environmental monitoring, among other domains. In this approach, spectral water indices including the Automated Water Extraction Index (AWEI), Water Ratio Index (WRI), Modified Normalised Difference Water Index (MNDWI), and Normalised Difference Water Index (NDWI) are crucial. They are essential tools for managing water resources and environmental monitoring because of their capacity to distinguish water from other forms of land cover and their adaptability to a variety of satellite sensors. These spectral water indices, like NDWI, MNDWI, WRI, and AWEI, have been shown by researchers to be useful in precisely distinguishing water bodies from other types of land cover. These indices take advantage of the distinct spectral characteristics of water, enabling precise and automated water extraction procedures in a variety of settings. Their versatility to be applied to various satellite sensors, such as Landsat TM, ETM+, and OLI, renders them adaptable instruments for detecting and tracking water bodies. The importance and use of these indices in the extraction of water bodies are covered in depth below.

3.6.1. Normalized Difference Water Index (NDWI)

The following equation represents the NDWI as presented by Mcfeeters, (1996): The modified NDWI For Landsat 5TM, ETM+7 and OLI data;
NDWI= (Green – NIR) / (Green + NIR)

$$NDWI = \frac{Band\ 2 - \ Band\ 5}{Band\ 2\ + \ \ Band\ 5} \quad or \quad \frac{Green - \ SWIR1}{Green + \ \ SWIR1}$$

For Landsat 8 OLI data;

$$MNDWI = \frac{Band\ 3 - \ Band\ 6}{Band\ 3\ + \ \ Band\ 6} \quad or \quad \frac{Green - \ SWIR1}{Green + \ \ SWIR1}$$

where NIR denotes a near infrared band and Green denotes a green band, such as TM band 4, OLI/TIRS band 5, and TM band 2, respectively. Using green wavelengths, this index aims to: (1) maximise water reflectance; (2) minimise low NIR reflectance by water features; and (3) capitalise on high NIR reflectance by vegetation and soil features. Water characteristics in this result have positive values, while soil and vegetation feature typically have zero or negative values. The Normalized Difference Water Index (NDWI) is a remote sensing index used to detect water bodies based on spectral reflectance differences. It is effective in distinguishing water bodies from other land cover types due to its unique spectral properties. NDWI is sensitive to variations in water content, making it useful for monitoring changes in water levels or seasonal fluctuations. It is simple to calculate, applicable across various satellite sensors, and provides a quantitative assessment. However, it can be affected by atmospheric conditions, adjacent land cover, seasonal variations, resolution limitations, and the need for contextual interpretation. Despite these limitations, NDWI remains a valuable tool for water body detection and monitoring.

3.6.2. Modified Normalized Difference Water Index

The modified Normalized Difference Water Indexs (MNDWI) for Landsat 5TM, ETM+7 and OLI data;

$$MNDWI = \frac{Band\ 2 - \ Band\ 5}{Band\ 2\ + \ \ Band\ 5} \quad or \quad \frac{Green - \ SWIR1}{Green + \ \ SWIR1}$$

For Landsat 8 OLI data;

$$MNDWI = \frac{Band\ 3 - \ Band\ 6}{Band\ 3\ + \ \ Band\ 6} \quad or \quad \frac{Green - \ SWIR1}{Green + \ \ SWIR1}$$

The maximum value in MNDWI is +1, while the lowest number is -1. The classification threshold is set at 0. where MIR is a middle infrared band and TM band 5, OLI/TIRS band 6 are examples of middle infrared bands, and green is a green band, such as TM band 2. Three outcomes were obtained from the MNDWI computation: Because it absorbs more MIR light than NIR light, water has higher positive values than those found in the NDWI. Built-up land, on the other hand, has negative values as previously mentioned. Finally, soil and vegetation have negative values because the former reflects MIR light more than NIR light and the latter still does so more than green light.

The Modified Normalized Difference Water Index (MNDWI) is a remote sensing index used to improve water detection in satellite imagery. It enhances contrast between water bodies and built-up land, effectively suppressing noise. MNDWI can be calculated using data from various satellite sensors, making it versatile for different applications and scales. It is effective across different geographic regions and environmental conditions, making it useful for global water body mapping and monitoring. Its simple formula makes it easy to implement and integrate into automated workflows for large-scale analyses. It can be used for temporal monitoring, assessing seasonal variations, drought impacts, and long-term trends. However, it is sensitive to atmospheric conditions, can struggle with mixed pixels, and depends on spectral bands. It may also be susceptible to temporal inconsistencies, potential misclassification, and calibration requirements.

3.6.3. Water Ratio Index (WRI)

The WRI proposed by (Shen & Li, 2010) is expressed the equation shown below

For Landsat 5TM and 7 ETM+ data;

$$WRI = \frac{Green + Red}{NIR + SWIR1} \quad Or \quad \frac{Bamd\ 2 + Band3}{Band\ 4 + Band\ 5}$$

For Landsat 8 OLI data;

$$WRI = \frac{Green + Red}{NIR + SWIR1} \quad Or \quad \frac{Bamd\ 3 + Band\ 4}{Band\ 5 + Band\ 6}$$

The water body's value exceeds one. TM band 2, OLI/TIRS band 3, red, TM band 3, OLI/TIRS band 4, NIR, Mid-IR, and SWIR are examples of infrared bands, Mid-Wave Infrared bands, and short-wave infrared bands, respectively. The WRI approach improved water while suppressing clouds, shadows cast by roads, and vegetation, and produced compelling findings for values greater than.

The Water Ratio Index (WRI) is a remote sensing index used for detecting water bodies in satellite imagery. It offers high sensitivity, enhanced contrast, and a straightforward calculation formula. It is easy to implement, versatile across different sensors, and suitable for long-term water dynamics studies. However, it can be influenced by vegetation and soil effects, atmospheric conditions, and mixed pixels. WRI requires specific spectral bands, which may not be available in all satellite sensors or vary in spatial or temporal resolution. Validation needs include ground truth validation, which can be labor-intensive and costly, and temporal variability, which can complicate the interpretation of long-term trends in water bodies. Overall, WRI is suitable for detecting and monitoring water bodies.

3.6.4. Automated Water Extraction Index (AWEI)

The AWEI proposed by Feyisa et al., (2014), is expressed as equation below;

$$AWEInsh = 4 * (Green - SWIR1) - (0.25 * NIR + 2.75 * SWIR2)$$

where NIR is a near infrared band and TM band 4, OLI/TIRS band 5, and green is a green band like TM band 2, OLI/TIRS band 3. Mid-infrared (MIR) bands include TM band 5, OLT/TIRS band 6, and short-wave infrared (SWIR) bands include TM band 7, OLI/TIRS band 8, and so on. The Automated Water Extraction Index (AWEI) is a remote sensing index designed for automated detection and extraction of water bodies from satellite imagery. It offers improved water detection accuracy, reduced false positives, and robustness across various conditions. It can be integrated with multiple satellite platforms, facilitating large-scale water body mapping and monitoring efforts. AWEI also allows for automated processing and analysis of large volumes of satellite imagery, reducing time and effort required for detection. It is effective in complex landscapes, particularly in urban and vegetated areas. However, AWEI's dependencies on specific spectral bands, sensor limitations, sensitivity to atmospheric conditions, complexity of implementation, mixed pixels, ground truth validation, and temporal variability can all pose challenges. Overall, AWEI is a valuable tool for monitoring water body trends and assessing environmental conditions. Regarding the AWEI, according to Reference (Feyisa et al., 2014), select AWEInsh for the village water, and both AWEIsh and AWEInsh for the city site in this study. This is because the village site met the condition that shadows were not a significant issue, while the city site met the condition that both high albedo surfaces and shadow/dark surfaces were present. The value 0 was used as the alternative threshold for AWEI imagery.

3.7. Extraction of Surface Water

Finchaa Lake surface water body was retrieved using NDWI, MNDWI, WRI, and AWEI. After that, the computed water indices were divided into two further classes: those with positive values denoted water bodies, and those with negative values, non-water surfaces

(Tesfaye & Breuer, 2023). Using raster calculators, the areas covered by water and non-water were determined for the years 1990, 2000, 2012, and 2022

Table 3-3 Satellite-derived indexes used for water features extraction in Landsat imagery

Multiband index	Equation	Remark	Reference
NDWI	NDWI = (NIR-Red) / (NIR + Red)	positive value	(Mcfeeters, 1996)
MNDWI	MNDWI = (Green - SWIRI) / (Green +SWIRI)	positive value	(Xu, 2006)
WRI	WRI = (Green + Red) / (NIR+SWIRI)	Water value is > 1	(Shen & Li, 2010)
AWEI	AWEI = 4*(Green - MIR) - (0.25*NIR + 2.75*SWIR)	positive value	(Feyisa et al., 2014)

Using the stratified random sampling method, in this study was selected 820 test samples (410 water and 410 non-water samples) to reflect the water and land features in the study area. The non-water samples are made up of soil, vegetation, and pixels from built-up areas, whereas the water samples are made up of pixels from rivers, lakes, and seas. The accuracy rating has been validated through the use of Google Earth and original satellite imagery. By employing NDWI, MNDWI, WRI, and AWEI water indices and dividing them into positive and negative classes, researchers were able to accurately delineate Finchaa Lake surface water body from satellite imagery. The subsequent determination of water and non-water areas using raster calculators provided valuable insights into the dynamics of Finchaa Lake over multiple time periods, contributing to a comprehensive understanding of water resources in the study area.

Table 3-4strength, limitation and best application of indexes used for water features extraction

strength, limitation and best application of indexes used for water features extraction

Index	Strengths	Limitations	Best Applications
AWEI	High accuracy in distinguishing water bodies from other surfaces. Effective in urban areas with complex backgrounds.	May require fine-tuning for specific environments. Sensitive to certain types of vegetation and soil moisture.	Identifying and delineating water bodies in urban and semi-urban areas.
MNDWI	Enhances open water features while suppressing built-up land, vegetation, and soil. Suitable for areas with sparse vegetation.	Less effective in densely vegetated or highly turbid water regions. Can misclassify certain non-water surfaces as water.	Mapping open water features in areas with low vegetation. Monitoring water extent changes in lakes and reservoirs.
NDWI	Good for identifying water bodies and suppressing noise from	Can be influenced by vegetation and built-up areas. Less effective in	General water body detection and monitoring. Analyzing

	built-up land and vegetation. Simple calculation using widely available bands.	turbid waters or areas with dense vegetation.	changes in surface water extent.
WRI	Effective in differentiating water from other land cover types. Uses multiple spectral bands to enhance water detection accuracy.	May be less effective in areas with high turbidity or mixed land cover. More complex to calculate compared to simpler indices.	Comprehensive water resource management. Suitable for detailed studies involving multiple land cover types.

3.8. Land use/land cover

The supervised image classification was done using ERDAS IMAGINE to create the land use land cover map of the study area. The images were obtained from http://earthexplorer.usgs.gov/, and the polygons for the vegetation area and other classes were created. Based on the spectral characteristics of satellite imagery and existing knowledge of land use in the around of study area, six LULC groups were defined and categorized for 1990, 2000, 2012, and 2022. In the study area, the following classes were identified: waterbody, agricultural, built up, grassland, forest, and swamp land. LULC in the study area was identified and classified. This comprehensive classification effort not only facilitated the identification and mapping of various land cover types but also provided valuable insights into the dynamics of land use and land cover changes over time. Such detailed LULC maps serve as indispensable tools for informed decision-making processes related to land management, environmental conservation, and urban planning endeavors within the study area and beyond.

Table 3-5 Land use and land cover classes

LULC class	Description
Water bodies	Regions that include surface water in the form of lakes, ponds, streams, rivers, and their principal tributaries
Grazing land	Grazing areas with grass covering as well as bare areas with little to no grass cover. It also comprises other species of tiny plants.
Agricultural land	Regions that are utilised for the annual and perennial production of crops. It is the region where the crops were collected, complete with standing crops, tree crops, and crop lands.
Forest land	Land covered with dense trees which are mainly ever green forest land
Swamps land	Swamps are forested wetlands near rivers or lakes, with slow-draining mineral soil and trees and bushes, and may have water year-round or part-year.
Built-up	Infrastructures made by human being such as roads, buildings, and settlement.

3.9. Accuracy Assessment

In this study, two images are used to assess the correctness of the data derived from the water indices method and the reference water body image. This is accomplished by creating 820 random points from the reference image, which are then exported as a "kml" file to be seen on "Google Earth." Each point is assessed separately to ascertain if it belongs in the "water" or "non-water" class. Finally, a % has been supplied to show the accuracy of the output (Ismail et al., 2022). The commaan accepted kappa coefficient and overall accuracy range

- < 0; agreement.
- 0.01 - 0.02; slight agreement
- 0.21 – 0.40; fair agreement.
- 0..41 – 0.60; Moderate agreement.
- 0.61 – 0.80; Substantial agreement.
- 0.81 – 1.00; Almost perfect agreement

In the study, the accuracy of the water indices method was rigorously evaluated by comparing its results with a reference water body image. This assessment involved several steps:

Reference Data Collection: A reference water body image was utilized as a benchmark for accuracy evaluation. From this image, 820 random points were systematically selected.

Point Assessment: Each random point was exactly analyzed to determine its classification as either "water" or "non-water." This assessment was conducted manually or aided by image processing software.

Export to Google Earth: The evaluated points were exported as a Keyhole Markup Language (KML) file, enabling visualization and analysis in Google Earth. This facilitated thorough verification and validation of the classifications.

Accuracy Metrics Computation: Various accuracy metrics were computed to quantitatively assess the performance of the water indices method. These metrics included:

Kappa Coefficient**:** A statistical measure of agreement between the classified results and the reference data, indicating the method's overall reliability.

$$K\text{appa Coefficient} = \frac{(\text{TC} * \text{TCS}) - \text{S}(\text{Column total} * \text{Row total})}{\text{TS}^2 - \text{S}(\text{Column total Row total})} * 100$$

Overall Accuracy: The proportion of correctly classified points (both water and non-water) relative to the total number of assessed points, providing a comprehensive measure of classification accuracy.

$$\text{Overall Accuracy} = \frac{\text{Total number of correctly classified pixels (Diagonal)}}{\text{Total numbr of reference pixels}} * 100$$

User Accuracy: The percentage of correctly classified water points out of all points classified as water, indicating the method's precision in identifying water bodies.

$$Users\ Accuracy = \frac{Number\ of\ correctly\ classified\ pixels\ in\ each\ category}{Total\ number\ of\ classified\ pixels\ in\ that\ category\ (the\ row\ total)} * 100$$

Producer Accuracy: The percentage of correctly classified water points out of all points that actually represent water in the reference data, reflecting the method's ability to accurately detect water.

$$Producer\ Accuracy = \frac{Number\ of\ correctly\ classified\ pixels\ in\ each\ category}{Total\ number\ of\ reference\ pixels\ in\ that\ category\ (the\ column\ total)} * 100$$

The study achieved a robust assessment of the efficacy of the water indices approach in accurately identifying water bodies by performing a thorough evaluation of the method against the reference data and computing these accuracy metrics. This thorough evaluation technique boosts confidence in the generated results by offering insightful information about the efficacy and dependability of the water body classification method.

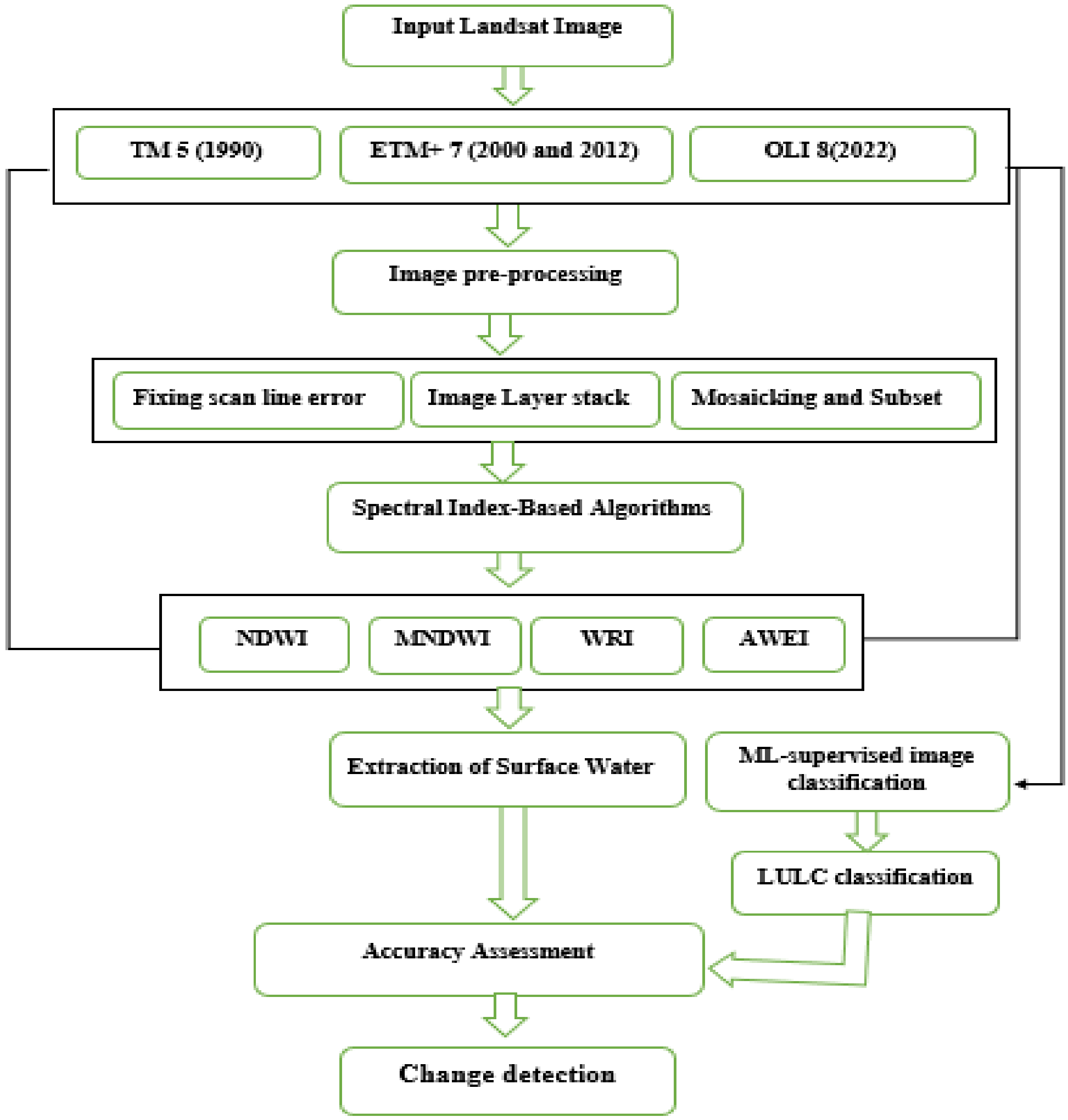

Figure 3-4 Flowchart showing the overall methods adopted in the study

4. RESULTS AND DISCUSSION

4.1. Evaluation of Water Indices performance

From Landsat TM, ETM, and OLI data, the efficiency of all of the NDWI, MNDWI, WRI, and AWEI in extracting surface water was assessed. The extraction capacities of the indices and few water bodies that were extracted using the NDWI, MNDWI, WRI, and AWEI. Thus, in this extensive water identification experiment using Landsat data in Google Earth, the MNDWI and AWEI are the best-performing water indices from a visual assessment standpoint for surface water detection. Presents accuracy indicators together with the accuracy estimates of each water index. Regarding the overall accuracy, producer's accuracy, user's accuracy, and Kappa coefficient, all indices have a satisfactory classification accuracy of >0.83. With an accuracy score of 0.85 overall and a Kappa coefficient of 0.83, this index is the least accurate of the group. Table 4.1 presents the performance of different water indices, providing information on their reliability and effectiveness. The MNDWI (Modified Normalised Difference Water Index) exhibits the best overall accuracy (97.5%) and kappa coefficient (0.97), demonstrating its superior ability to identify different types of water. The AWEI (Automated Water Extraction Index) also demonstrates high accuracy, making it a dependable option. However, the Normalised Difference Water Index (NDWI) does not perform as well as the MNDWI and AWEI, as indicated by its lower accuracy and kappa coefficient (92.5% and 0.86, respectively). The Water Ratio Index (TWRI) has the lowest performance among all the assessed indices, with a kappa coefficient of 0.83 and an overall accuracy of 85%. These findings highlight the limitations of WRI in precisely identifying water bodies, due to its sensitivity to specific land cover types and atmospheric factors. Therefore, it is important to carefully select indices based on the unique characteristics of each research topic.

Table 4-1 Overall accuracy and kappa coefficient of the spectral indices in four test dates.

	07/01/1990		27/01/2000		12/01/2012		31/01/2022	
	OA (%)	kappa	OA (%)	kappa	OA (%)	kappa	OA (%)	Kapp a
NDWI	92.5	0.87	93	0.86	93.5	0.89	94.4	0.89
MNDWI	97.5	0.95	96	0.94	97	0.93	97.8	0.93
WRI	85.0	0.83	90	0.86	92	0.87	93.5	0.89
AWEI	95.5	0.93	97	0.95	95	0.92	97.6	0.93

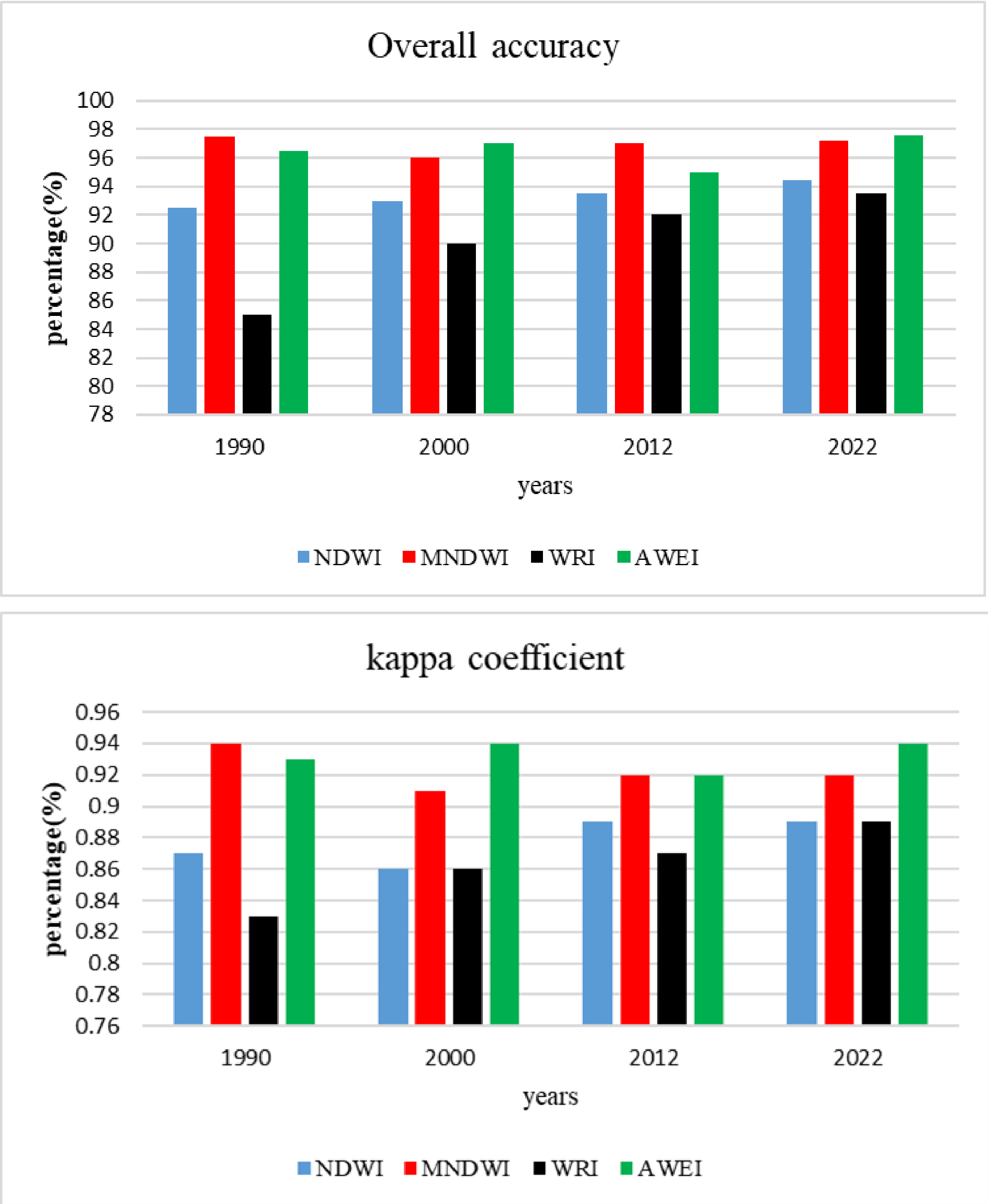

Figure 4-1 Analysis of the Kappa Coefficient and overall accuracy using four different algorithms

As regards surface water detection, both the MNDWI and AWEI showed good performances; however, few outliers were detected. The results indicated that the MNDWI and AWEI water indices were the most accurate. This was also observed in case studies conducted in Switzerland, Ethiopia, South Africa, and New Zealand, where AWEI achieved water user's and producer's accuracies ranging from 96% to 99% and 91% to 99% respectively (Feyisa et al., 2014). Additionally, AWEI demonstrated high accuracy in a shadow-free image from Denmark, with water user's and producer's accuracies of 98% and 92% respectively (Feyisa et al., 2014). Similarly, According to (Ali et al., 2019a), MNDWI and AWEI provide a more detailed analysis of water surface detection than NDWI. MNDWI and AWEIsh performed best, NDWI and WRI performed less accurately, and WRI performed the least, according to Asfaw et al., (2020). The evaluation criteria used in this study are widely accepted for assessing surface water detection results using water indices (Feyisa et al., 2014; Xu, 2006). In this study, the MNDWI accurately predicted surface water areas of 182.13 km^2, 173.98 km2, and 197.25 km2 in 1990, 2012, and 2022 respectively. AWEI also accurately predicted a surface water area of 190.08 km2 in Fincha Lake in 2000. The MNDWI and AWEI demonstrate good accuracy and kappa coefficients, making them reliable choices for surface water detection, especially in areas where accurate mapping of water bodies is essential. Future investigations can focus on enhancing the performance of these indices, exploring combinations of different indices for improved accuracy, and testing them in various regions and climate scenarios to ensure their resilience and applicability.

4.2. Estimated Surface area Changes from the MNDWI and AWEI

Water indices, such as MNDWI and AWEI, are used to determine the extent and dynamics of surface water in Finchaa Lake. These indices, derived from raster calculation techniques and Landsat satellite imagery, help identify long-term trends and patterns in surface water dynamics. These indices provide a comprehensive understanding of Finchaa Lake's hydrological features, enabling informed decision-making for water resource management and conservation initiatives. These insights are crucial for sustainable lake management and understanding the lake's response to environmental changes. A threshold value was used throughout the investigation to distinguish between land and water areas. Various threshold values were observed in the water index images based on the time intervals and type of water index (Ali et al., 2019b). As to Ibrahim & Al-fugara, (2022) there is a known difference in value between the water pixels and other land cover areas; the former having higher values. When the pixel water area was compared to the nearby land cover types, it was found to have significantly higher MNDWI and AWEI threshold values. In general, it was found that the water threshold values based on the MNDWI and AWEI were higher than 0.1. Table 4.2 shows changes in lake surface water bodies during four years in lake surface water bodies of fincha lake from 1990 to 2022.

Table 4-2 Estimated Surface area Changes from the MNDWI and AWEI

Year	Surface Area (MNDWI) in km2	Surface Area (AWEI) in km2
1990	182.13	187.84
2000	189.08	190.08
2012	173.98	176.98
2022	197.25	194.21

The surface area of the lake has consistently increased according to both the MNDWI and AWEI over the specified time period, demonstrating the accuracy of these indices in identifying changes in the water body. Although the two indices show comparable trends, their sensitivity to particular climatic elements and noise levels could lead to small variations in the projected surface areas. Because it can reduce built-up noise, MNDWI may be more susceptible to water in urban settings, but AWEI is made to withstand a variety of environmental factors, such as shadows and populated areas. In result, measuring surface area changes with MNDWI and AWEI offers important insights into the dynamics of water bodies. These indices are essential for comprehending temporal shifts, which helps with efficient water resource management and conservation.

4.2.1. Modified Normalized Difference Water Index (MNDWI)

The lake surface water bodies were extracted by Modified Normalized Difference Water Index (MNDWI) from Landsat satellite. The images were then classified into two categories consisted of water and non-water objects. The lake water body was extracted by Modified Normalized Difference Water Body because this method more suitable for increasing the accuracy of water extraction and effectively reduce as well as remove built-up land noise than NDWI. Furthermore, MNDWI can be concluded more detail detecting urban water surface than NDWI (Xu, 2006). The MNDWI images are classified as either non-water or water using a zero threshold. 0.9 (1990), 0.68 (2000), 0.73 (2012), and 0.25 (2022) are the MNDWI threshold values for each year. Table 4.2. Surface water bodies' areal extent (in km2) of MNDWI for years 1990-2022. The result of Modified Normalized Difference Water Index (MNDWI) shows that the lake surface water bodies of fincha lake have been experiencing fluctuation from 1990 to 2022.

Table 4-3 Surface water bodies' areal extent (in km2) of MNDWI for years 1990-2022

Year	Index's	min threshold	max threshold	Water body
1990	MNDWI	-0.61	0.90	182.13
2000	MNDWI	-0.47	0.68	189.08
2012	MNDWI	-0.48	0.73	173.98
2022	MNDWI	-0.36	0.26	197.25

The distribution of lake surface water bodies in fincha lake based on MNDWI analysis can be seen in following figure 4.2. Modified Normalised Difference Water Body was used to remove the Lake water body because it is a more accurate method than NDWI for boosting the accuracy of water extraction and for efficiently reducing and removing built-up land noise.

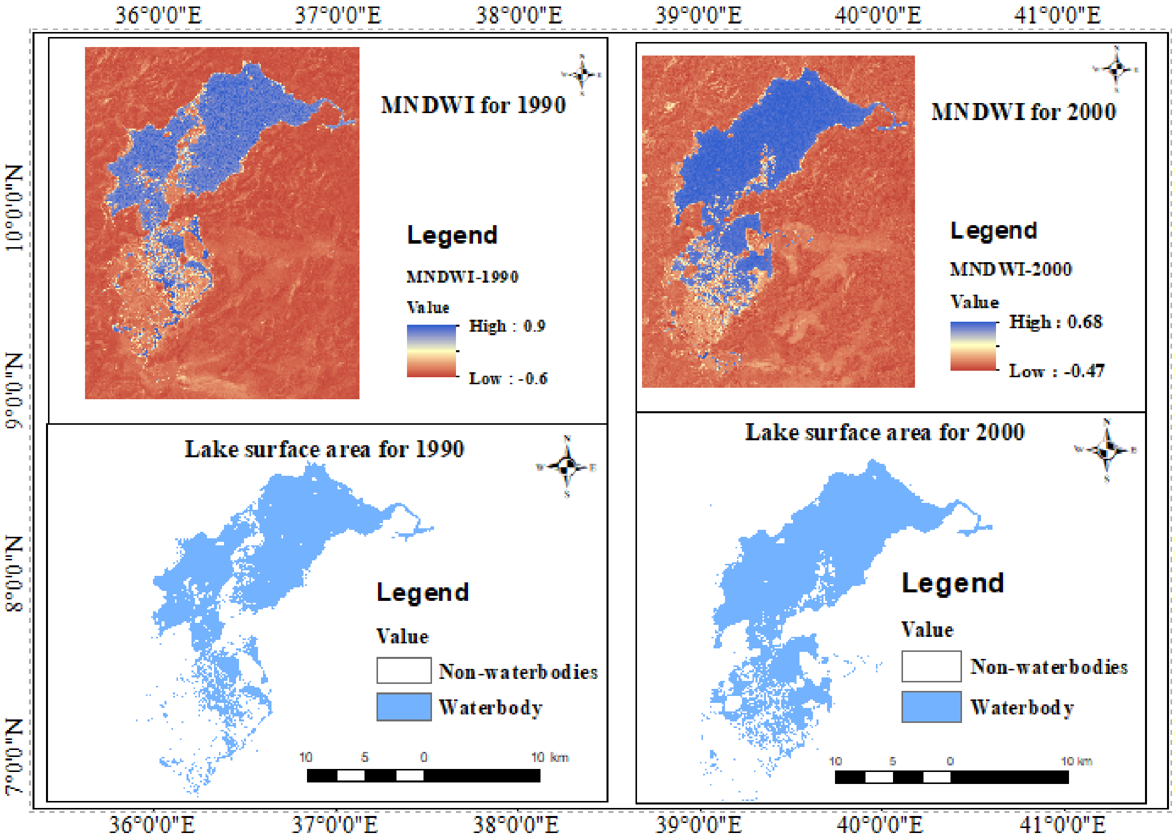

Figure 4-2 MNDWI images extracted surface water body for 1990 and 2000

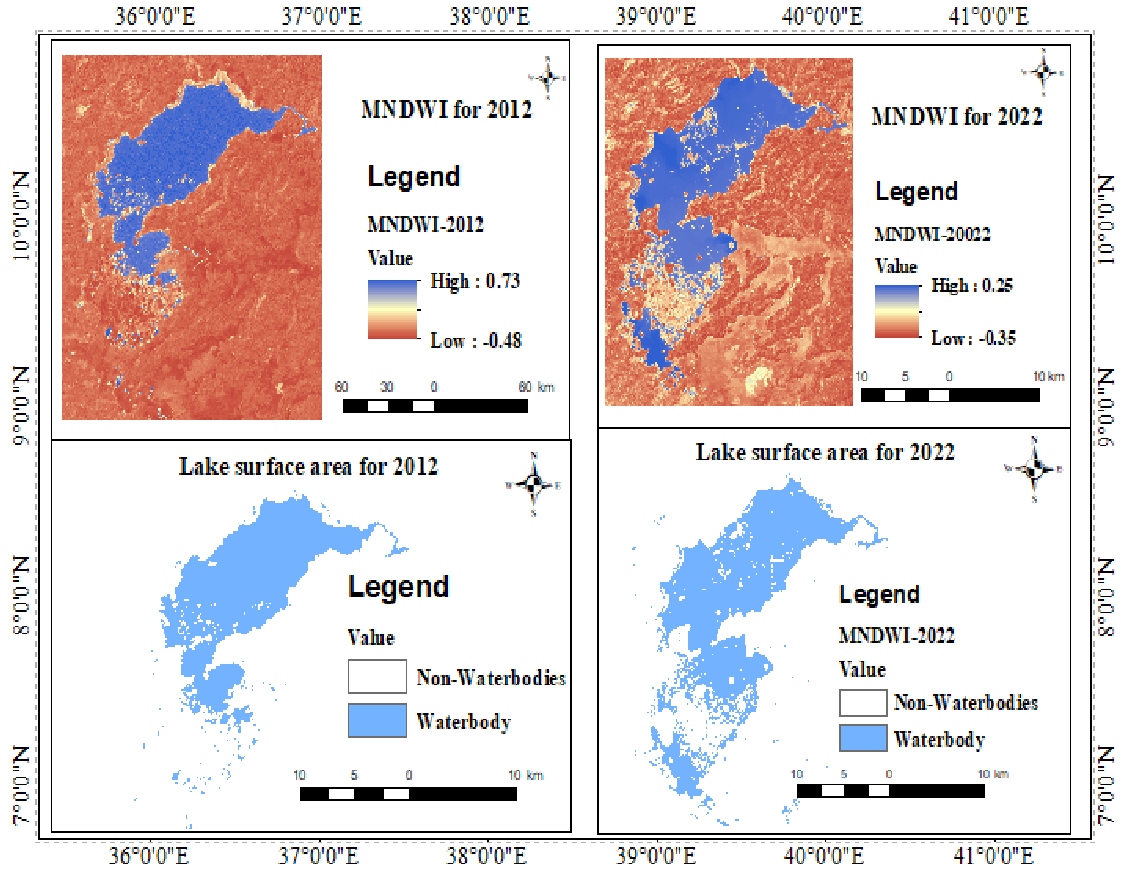

Figure 4-3 MNDWI images extracted surface water body for 2012 and 2022

In the Modified Normalised Difference Water Index (MNDWI), Xu (2006) proposes that the Near Infra-Red band be replaced with the Middle Infra-Red band in order to reduce noise from vegetation and populated areas. Due to their tendency to produce negative MNDWI values, this adjustment makes it easier to remove such noise. Table 4.3 displays the estimated MNDWI values for the aforementioned years, and Figure 4.2 shows the classified bodies of water together with the MNDWI indices for the dry seasons of 1990, 2000, 2012, and 2022. But, as with the Water Ratio Index (WRI) method, MNDWI use is limited to images that have the Middle Infra-Red band, therefore it only covers data from 1990, 2000, 2012, and 2022.The MNDWI images are classified as either non-water or water using a zero threshold. 0.9 (1990), 0.68 (2000), 0.73 (2012), and 0.25 (2022) are the MNDWI threshold values for each year. The MNDWI is an effective tool for differentiating between water and non-water objects since it typically yields values over zero in water areas and significant negative values in vegetation areas. Especially in places where Middle Infra-Red band data is accessible, this method makes precise water body delineation possible and aids in tracking variations in water extent over time.

4.2.2. Automated Water Extraction Index (AWEI)

Accurately identifying water bodies in environments with shadows and dark surfaces was made possible by the Automated Water Extraction Index (AWEI). AWEI is a surface water and surrounding terrain distinguishing technology that was developed primarily to suppress shadow pixels and improve water extraction precision. All the details of the AWEI threshold values and how they impact the recognition of water bodies are given in Table 4.4 and Figure 4.3.

Table 4-4 Surface water bodies' areal extent (in km2) of AWEI for years 1990-2022

Year	Index's	min threshold	max threshold	Water body
1990	AWEI	-2.54	0.25	187.84
2000	AWEI	-1.38	0.18	190.08
2012	AWEI	-1.37	0.14	176.98
2022	AWEI	-0.9	0.91	194.21

The MNDWI images are classified as either non-water or water using a zero threshold. 0.25 (1990), 0.18 (2000), 0.14 (2012), and 0.91 (2022) are the AWEI threshold values for each year. Different conclusions were drawn from the AWEI examination of Landsat images taken in January 1990, 2000, 2012 and 2022. As a result, the water areas in January were measured at 187.84, 190.08, 176.98, and 194.21 square kilometres, respectively. These results highlight how crucial it is to use specialised indices, such as AWEI, for accurate water body extraction, especially in areas with difficult environmental conditions. The efficacy of AWEI in tracking alterations in aquatic environments over an extended period is evidenced by its reliability and precision over several years, offering significant perspectives for the management of water resources and preservation initiatives in the Finchaa area. According to Zhai et al. (2015), the AWEI can distinguish water features from shadows and high-albedo geographic features compared to the MDWI and NDWI. The size of the lake increased by 4% between 1990 and 2000, decreased by 8% between 2000 and 2012, then increased by 13% between 2012 and 2022.

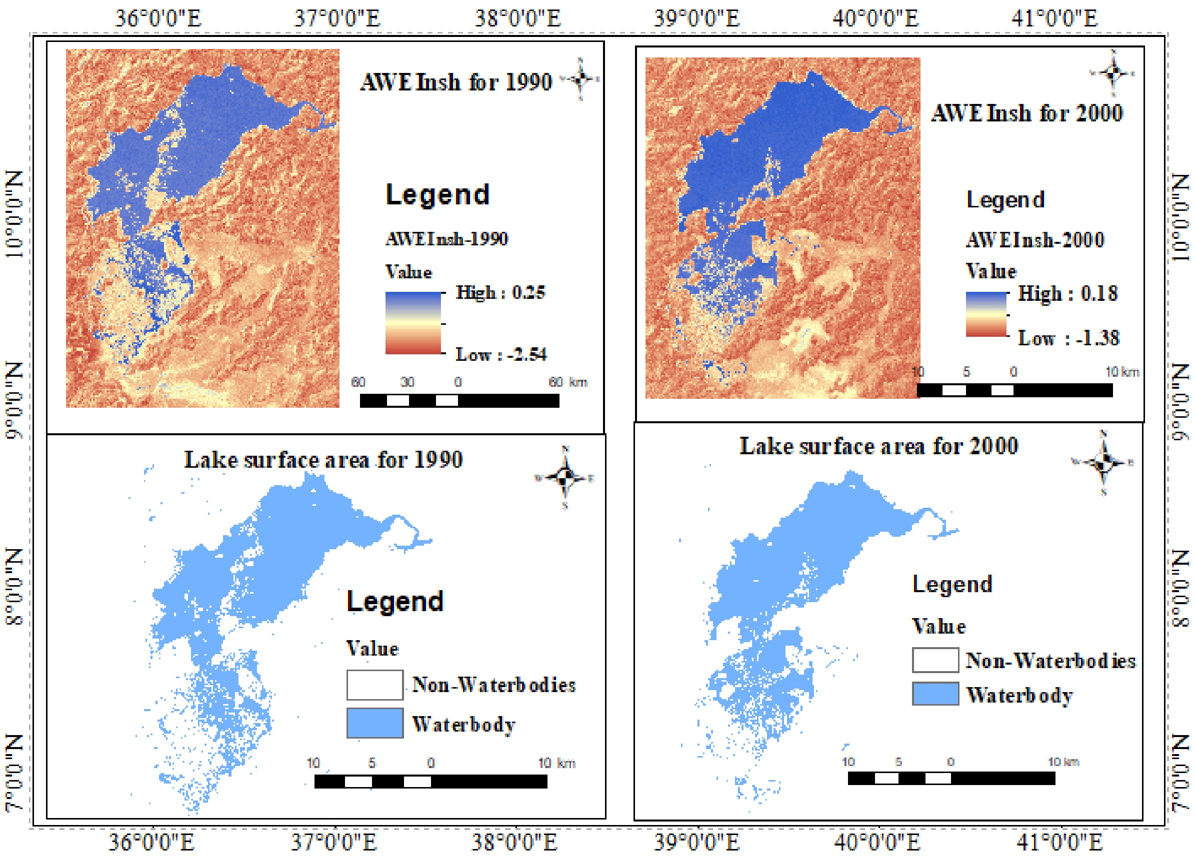

Figure 4-4 AWEI images extracted surface water bodies for 1990 and 2022

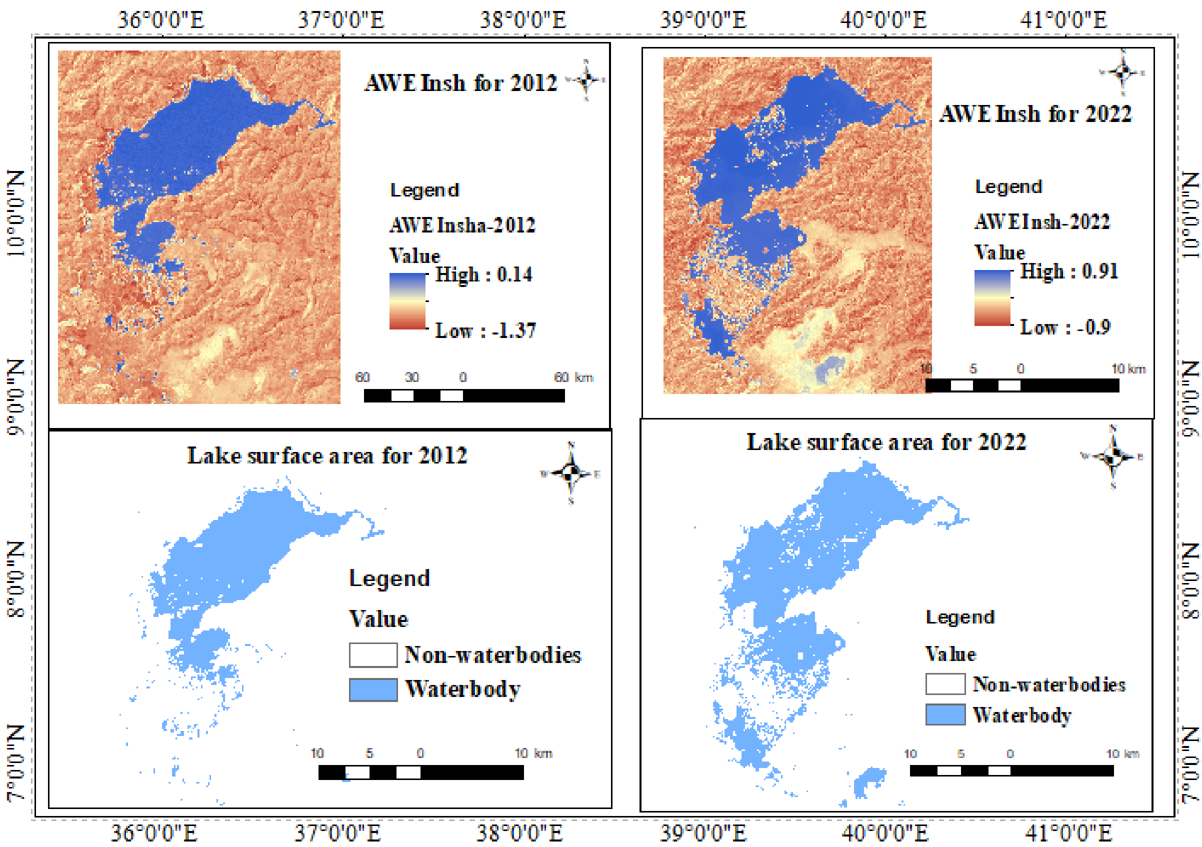

Figure 4-5 AWEI images extracted surface water bodies for 2012 and 2022

In this investigation, the Automated Water Extraction Index (AWEI) showed to be an effective tool for extracting water features, especially in locations with dark surfaces and shadows. AWEI is designed to suppress shadow pixels in order to improve surface water extraction accuracy. However, as the Normalised Difference Moisture Index (NDMI) was created to measure the moisture content of plants, it was not appropriate for the extraction of water features in the Finchaa region. Informed decision-making for water resource management and environmental conservation initiatives is made possible by the extracted water area data, which is an essential tool for evaluating changes in water availability and distribution. MNDWI and AWEI outperformed other indices in terms of extracting water pixels from Landsat data, according to the results of the error matrix and water indexing. Because no built-up land patches were combined with enhanced water features, the water information from the MNDWI has an overall accuracy of 91% to 97% and a Kappa value of 0.91 to 97.5. The study overall findings underline the significance of using suitable remote sensing indices for water feature extraction and the important contribution of AWEI to improving water mapping accuracy under difficult environmental circumstances. These discoveries strengthen this knowledge of the Finchaa region water dynamics and aid in the management of water resources in a way that will benefit present and future generations.

4.3. Analysis of the Surface Area of the Lake

The lakes surface water area was determined using the AWEI 2000 (ETM+), Modified Normalised Difference Water Index (MNDWI) for 1990 (TM), 2012 (ETM+), and 2022 (OLI_TIRS), as well as Nonetheless, the Fincha Lake's water surface areas have shown a number of rises and falls over the years. The lake's water surface area, for example, declined between 2000 and 2012 before progressively increasing until 2022. The lake's area shrank sharply until 2012, at which point it began to increase until 2022. Based on the variations in the lake surface area, the largest lake area was recorded in 2022 at 197.25 km^2, while the smallest area was recorded in 2012 at 173.98 km^2. Fincha Lake's average water surface area is approximately 185.61 km^2. The area of the lake dropped from 189.08 km^2 in 2000 to 15.1km^2 in 2012. The lake's area has increased by 23.27 km^2 during the past 32 years, according to long-term monitoring of its water surface area. AWEI research conducted in January 2022 using Landsat OLI imagery showed that the area covered by water was 194.21square kilometres, whereas the amount covered by land was 756.11 square kilometres. Higher precipitation, less water being used out for industrial or agricultural use, or other favorable hydrological circumstances could be the cause of the lake's area growth during this time (Chen & Duan, 2022). Many factors, including rising sedimentation (which reduces the lake's capacity) and climate change (which results in lower rainfall or greater evaporation rates), could have contributed to the significant decrease in surface water area between 2000 and 2012. Figure 4.5. displays lake imagery every four years from 1990 to 2022 in order to demonstrate a drop in the time series of the Fincha Lake's water surface areas as determined by the MNDWI and AWEI index from Landsat satellite data. The previous 32 years have seen significant changes to the lake's surface size and shape. AWEI and MNDWI were unable to get rid of the snow cover and shadows, according to Acharya et al. (2018). Nevertheless, choosing the ideal threshold increased the accuracy, though not appreciably. Therefore, according to Acharya et al. (2018) and Zhai et al. (2015), no single method could accurately extract the full water surface.

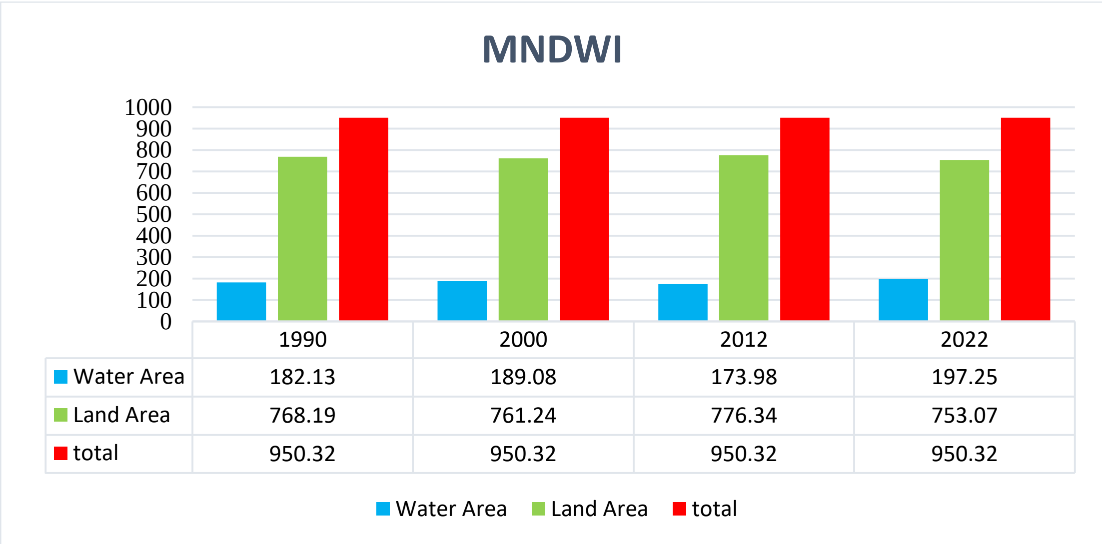

	1990	2000	2012	2022
Water Area	182.13	189.08	173.98	197.25
Land Area	768.19	761.24	776.34	753.07
total	950.32	950.32	950.32	950.32

Figure 4-6 Changed surface water area for MNDWI in different years

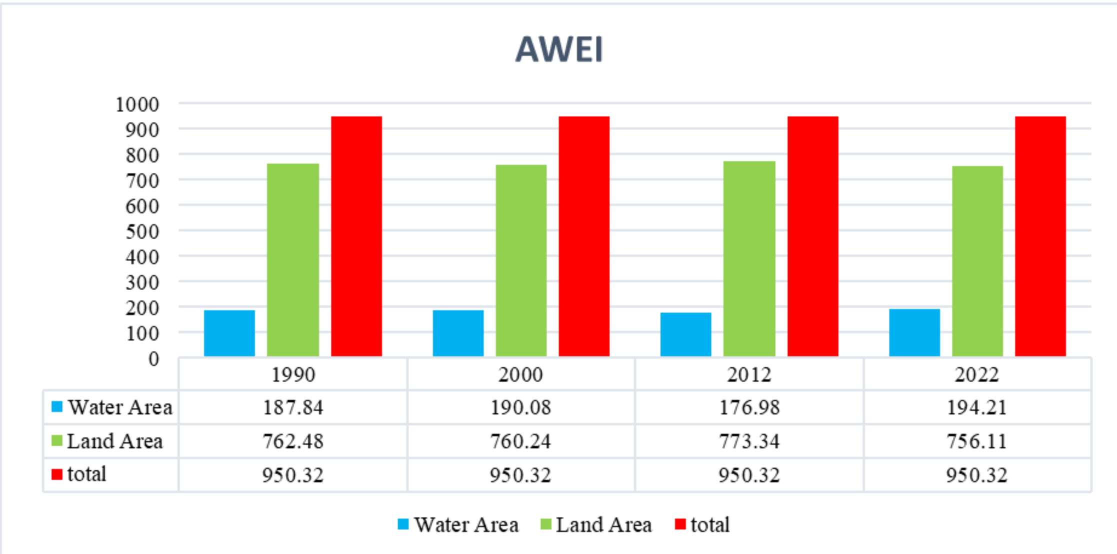

	1990	2000	2012	2022
Water Area	187.84	190.08	176.98	194.21
Land Area	762.48	760.24	773.34	756.11
total	950.32	950.32	950.32	950.32

Figure 4-7 Changed surface water area for AWEI in different years.

4.3.1. Evaluation of The Changes

Fincha Lake water area was extracted over four key periods (1990, 2000, 2012, and 2022) using spectral water indexing and ML-supervised classification techniques. Regrettably, the fluctuations of the surface water have changed significantly recently, and the surrounding grasslands and farms have grown more extensive, which has presented the lake with several challenges. Various water indices, including the Normalised Difference Water Index (NDWI), Water Ratio Index (WRI), Modified Normalised Difference Water Index (MNDWI), and Automated Water Extraction Index (AWEI), were examined. The findings demonstrated that the lake water area displayed a variety of patterns over time. The indicators showed that the lake water area changed very little between 1990 and 2000. On closer inspection, however, Figure 4.5 depicts a more notable change in the Lake water area between 2000 and 2012. This points to a time of significant environmental change that may be caused by alterations in land use, differences in the temperature, and human activity. The findings derived from NDWI, MNDWI, WRI, and AWEI offer significant understanding of Finchaa Lake surface area variations throughout various time periods. As shown in Table 4.6, the assessed surface area of the lake was measured in January 1990, 2000, 2012, and 2022 and was found to be 182.13 square kilometres, 189.08 square kilometres, 173.98 square kilometres, and 197.25 square kilometres, respectively.

During the period from 1990 to 2000, Figure A illustrates the changes in the lake's surface area. Generally, this decade may have shown trends of either expansion or contraction of the lake's surface area might be due to various factors such as climatic conditions, water inflow, and human activities. Specific details about the extent and direction of these changes would provide a clearer picture of the trends observed during this period. Figure B covers the period from 2000 to 2012. This period likely highlights different trends compared to the previous decade. There might be observable patterns indicating whether the lake continued to expand, contracted further, or stabilized. Changes during this time could be influenced by factors such as increased water usage, climatic variations, or environmental policies implemented to manage the lake's ecosystem. Figure C depicts the variations in the lake's surface area from 2012 onwards, with a notable significant change in the direction towards the southwest. This indicates a directional shift in the lake's expansion or contraction, possibly influenced by geographical features, water flow directions, or human interventions such as water management projects. The southwest direction change suggests a pronounced alteration in how the lake's surface area is evolving, which could be due to specific environmental changes or localized human activities impacting the southwest region more significantly. Across these three figures, one can observe how the lake's surface area has changed over more than two decades. These changes could be influenced by a combination of natural factors like precipitation, droughts, and river inflows, as well as anthropogenic factors such as dam constructions, water extraction, and land use changes around the lake. The significant shift towards the southwest in the most recent period might indicate new environmental or human pressures that are specifically affecting that region.

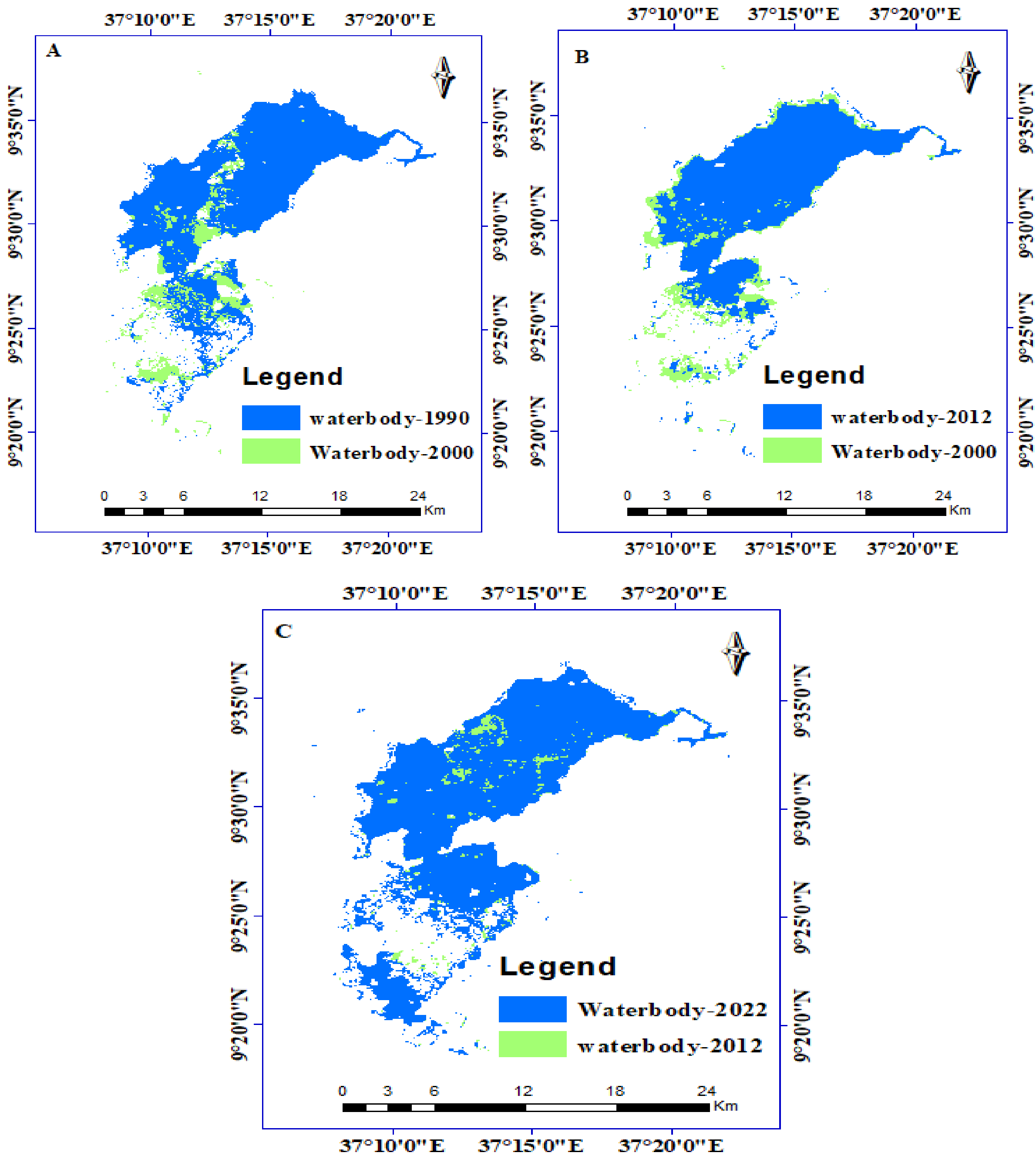

Figure 4-8 Evaluation of the changes of the lake.

According to the findings, the surface area of Fincha Lake in 1990 was around 182.13 square kilometres (Table 4.5). The surface area had increased by almost 7.95 square kilometers by the year 2000. Compared to that, the surface area of the Fincha Lake declined by around 16.1 square kilometers in 2012. In 2022 the surface area of the Fincha Lake increases by 23.27 square kilometers. Based on the meta information and observational evidence collected from the inhabitants and elders residing near the lake, it has been observed that the water surface area of the lake has significantly decreased. This phenomenon has been attributed to a prolonged drought that the region has experienced over the past years. The region's agricultural activities have risen, according to study findings and the Land Use and Land Cover (LULC) analysis carried out in 2022. More soil erosion as a result of the increase in agriculture has released more silt into the lake. The sedimentation increases the surface area of the lake by causing the water to spread outward. Nevertheless, the lake's total volume might have dropped in spite of this rise in surface area.

Between 1990 and 2000, the size of the lake experienced a 4% increase. This period marked a growth phase, possibly influenced by factors such as climate patterns, human interventions like irrigation, or natural cycles affecting water levels. Following this growth, from 2000 to 2012, there was an 8% decrease in the lake's size. This decline could be attributed to various factors, including prolonged droughts, increased water usage for agriculture or urban development, or altered water flow patterns due to environmental changes. From 2012 to 2022, the lake size rebounded with a 13% increase. This recovery phase might have been facilitated by improved rainfall patterns, conservation efforts, restoration projects, or changes in water management practices that aimed to replenish the lake's water levels. The fluctuation in the lake's size over these periods underscores the complex interplay of natural and human factors impacting aquatic ecosystems. Monitoring such changes is crucial for understanding environmental resilience and implementing sustainable water management strategies

Table 4-5 Statistics of the Lake Surface Area Changes

Year	Calculated lake area (in km2)	Variation of Lake surface area in between years (in km2)	Variation of Lake surface area in between base period/design year/ and year of predict ion (in km2)
From design document of lake	170		
1990	182.13		12.13
2000	190.08	7.95	19.08
2012	173.98	-16.1	3.98
2022	197.25	23.27	27.25

These data demonstrate the dynamic character of the lake environment and emphasise how crucial it is to continue management and monitoring activities in order to ensure the survival of the system. It is imperative to acknowledge the fundamental factors that give rise to the observed fluctuations in the water area of the lake.

Increases in grassland and agricultural regions around the lake might be a sign of shifting land uses, which could impact the way water flows, how much sediment settles there, and the health of the ecosystem as a whole. Furthermore, throughout time, climate fluctuations can have a major impact on lake dynamics and water availability (Islam & Mostafa, 2024). These variations include changes in temperature and precipitation patterns. In addition, decrease in forested areas resulted in increased soil erosion that negatively impacted the hillslopes in the basin and increased sediment yield in the river, which is currently creating issues in the Fincha hydroelectric reservoir(Regasa & Nones, 2022b).

4.4. Assessing land use and land cover change affecting the extent of Lake

Assessing land use and land cover (LULC) changes is crucial for understanding their impact on the extent of lakes and other water bodies. Remote sensing techniques, such as satellite imagery analysis, provide valuable tools for monitoring and assessing these changes over time. The best approach for analyzing LULC shifts that impact a lake's extent is to routinely examine satellite images of the lake and the surrounding area. The extent of the lake may be impacted directly or indirectly by changes in land cover types such as deforestation, agricultural expansion, and modifications to wetland regions, all of which can be identified by this (Dibaba et al., 2020a) Changes in land cover types, such as deforestation, agricultural development, and adaptations to wetland zones, can be observed through the analysis of satellite data. The size of lakes and other bodies of water may be impacted by these changes, either directly or indirectly. For example, deforestation, agricultural expansion, and wetland modification (changing wetland areas by drainage or filling can upset the hydrological balance of the lake's). These changes can directly or indirectly impact the extent of lakes and other water bodies.

4.4.1. Land use land cover Classification

The Maximum Likelihood supervised classification technique was used to extract the land-use and land-cover change in the Lake area of the research area from the images taken in the years 1990, 2000, 2012, and 2022. Maximum Likelihood classification was used because it reliably classified land cover classes and produced accurate results for additional research. Because land cover is dynamic, it was important to take changes over time into account instead of assuming constancy, which could result in misleading conclusions, particularly in the context of hydrological modelling. Six main classifications of land cover were identified as a consequence of the classification process: built-up, swamp, grassland, agricultural, forest, and waterbody environments. In order to enable an extensive investigation of landscape dynamics, these classes were selected to cover a wide range of land use forms that are frequently observed in the area around Finchaa Lake. The distribution of land and water was depicted in classified images created by the classification findings, which made it possible to calculate areas in square kilometres and percentages. The majority of the study region was made up of three main land cover classes: waterbodies, grasslands, and agricultural areas. The rise in the total lake area indicates that these data highlight notable changes in LULC patterns surrounding Finchaa Lake during the previous three decades. Table 4.6 shows the distribution of land cover types. Agricultural and grassland areas make up the highest amounts, followed by waterbodies, and built-up land area only makes up a small percentage of the total.

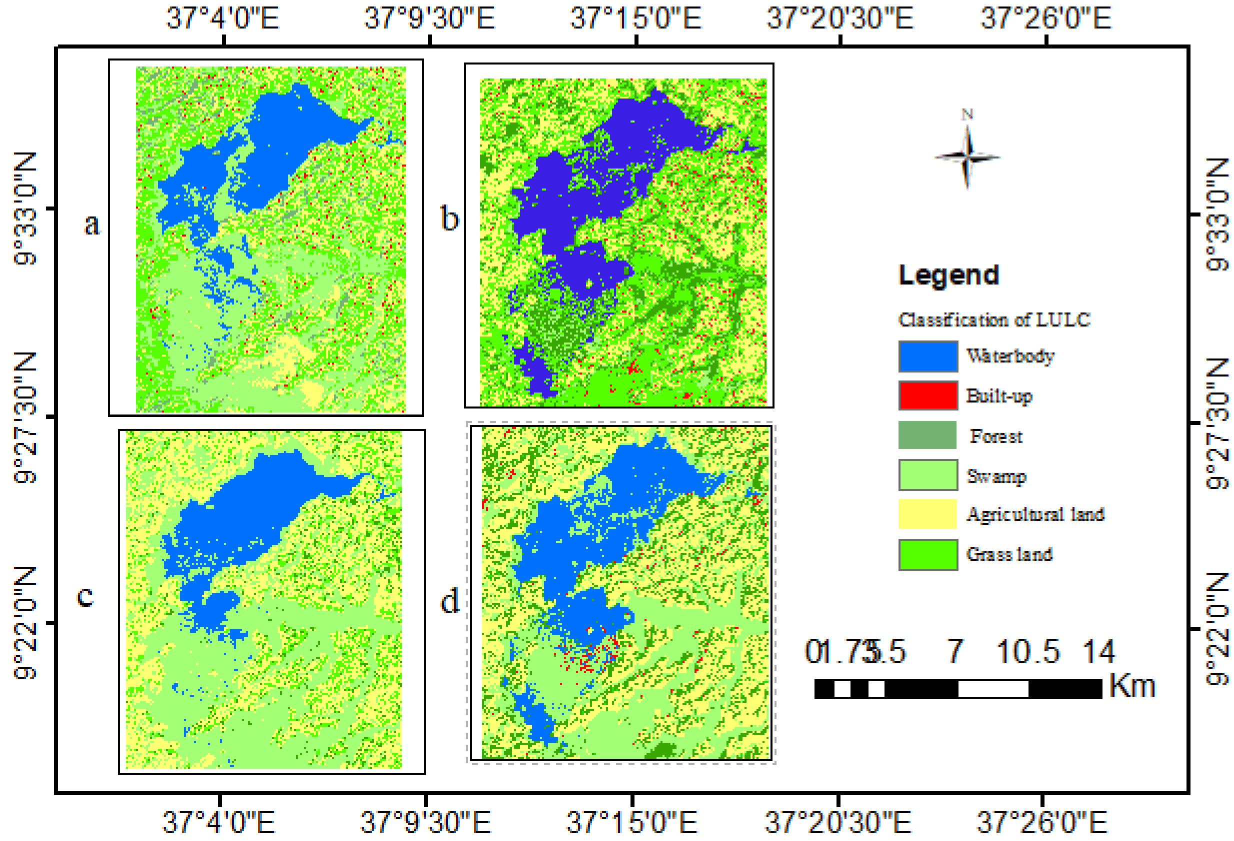

Figure 4-9 Classification of LULC Change in the Finchaa Lake

The Maximum Likelihood supervised classification technique was used to extract the land-use and land-cover change in the Lake area of the research area from the pictures taken in the years 1990, 2000, 2012, and 2022. Tables 4.6 display the outcomes. Between 1990 and 2000, this class experienced the greatest rate of change in the agricultural land area (27.38%) and water bodies (18.75%). Likewise, there is a change in the built-up area (1.44%), but the values of the forest, swamp, and grassland decreased by (-5.16), (-9.14%), and (-3.16%), respectively. With the exception of agricultural land and swamp areas (17.23%) and (9.44%), all other land coverings saw declines between 2000 and 2012, (-6.48%) for water bodies, (-0.92%) for forests, and (−6.48%) for water bodies. With the exception of Grass land and swamp areas (8.8%) and (18.23%), all other land coverings saw increased between 2012 to 2022.

Table 4-6 LULC around the Finchaa Lake between 1990 and 2022

Nameof classified	Area-1990(Km^2)	%	Area-2000(Km^2)	%	Area-2012(Km^2)	%	Area-2022(Km^2)	%
Waterbody	149.22	16.17	179.64	18.75	129.18	12.27	187.13	19.98
Agricultural	122.82	13.31	256.39	27.38	418.69	44.61	522.21	55.75
Forest	79.34	8.59	32.09	3.43	23.59	2.51	22.31	2.35
Built-up	5.88	0.64	13.47	1.44	17.68	1.63	19.01	1.96
Swamp	118.28	12.81	34.38	3.67	123.03	13.11	40.36	4.31
Grass land	447.57	48.49	424.54	45.33	256.77	27.36	85.69	9.15
Total	941.19	100.00	941.19	100.00	941.19	100.00	941.19	100.00

Accuracy evaluation was done after classification to confirm the dependability of the categorized maps. The classification findings showed a high degree of agreement between the categorized maps and reference data, with an overall accuracy of 95% and a kappa coefficient of 0.94. The robustness of the classification procedure and the precision of the generated LULC maps were guaranteed by this validation step. By analysing these maps over the selected years, the study provided insight into the temporal dynamics of land cover around Finchaa Lake. For land management plans, conservation efforts, and sustainable development projects in the area to be informed, it is imperative that these changes be understood. Thorough evaluations of this kind support in the preservation and efficient use of natural resources and help to evidence-based decision making.

4.4.2. Change detection analysis

In this, research for LULC, natural resource management, and environment monitoring & protection, the detection of land use and land cover change based on remote sensing pictures has been widely employed (Chen, 2023). Using ArcGIS software, ML-supervised categorised images for each year independently have been used to determine the percentage area of each land cover class. Across several LULC classes, positive as well as negative patterns have been noted. Positive values indicate a growing pattern in specific LULC categories, whereas negative values indicate a declining trend. Agricultural land has shown a growing trend over the course of the study, covering an area of 42.41 km^2. Furthermore, from 2000 to 2022, the area that was built up expanded by 1.32 km^2.

Furthermore, grassland decreased by (-3.16%), (-17.97%), and (-18.21%) in 2000, 2012, and 2022, respectively. In contrast, grassland and forest decreased by (-21.37%) and (-6.24%) from 2000 to 2022, respectively (Figure 4). Additionally, due to rapid human population growth, resettlement programs, climate change, and human and nature -induced driving forces were the main triggers of LULC change in sub-Saharan African countries, particularly in Ethiopia (Regasa, 2021). Additionally, in 2000, 2012, and 2022, grassland declined by (-3.16%), (-17.97%), and (-18.21%), respectively. Conversely, from 2000 and 2022, grassland and woodland saw declines of (-21.37%) and (-6.24%), respectively (Figure 4-8). Hailu et al., (2020) in the Jimma Geneti district and Kabite et al., (2020) in the Didessa River basin have both reported findings that are similar. According to Tewabe & Fentahun, (2020), the Tana basin's residential areas and agricultural land have grown dramatically over the last 32 years, by 8.05% and 15.61%, respectively. Furthermore, the primary causes of LULC change in sub-Saharan African nations, especially Ethiopia, were resettlement policies, climatic change, and human and natural pressures produced by population expansion (Regasa, 2021),

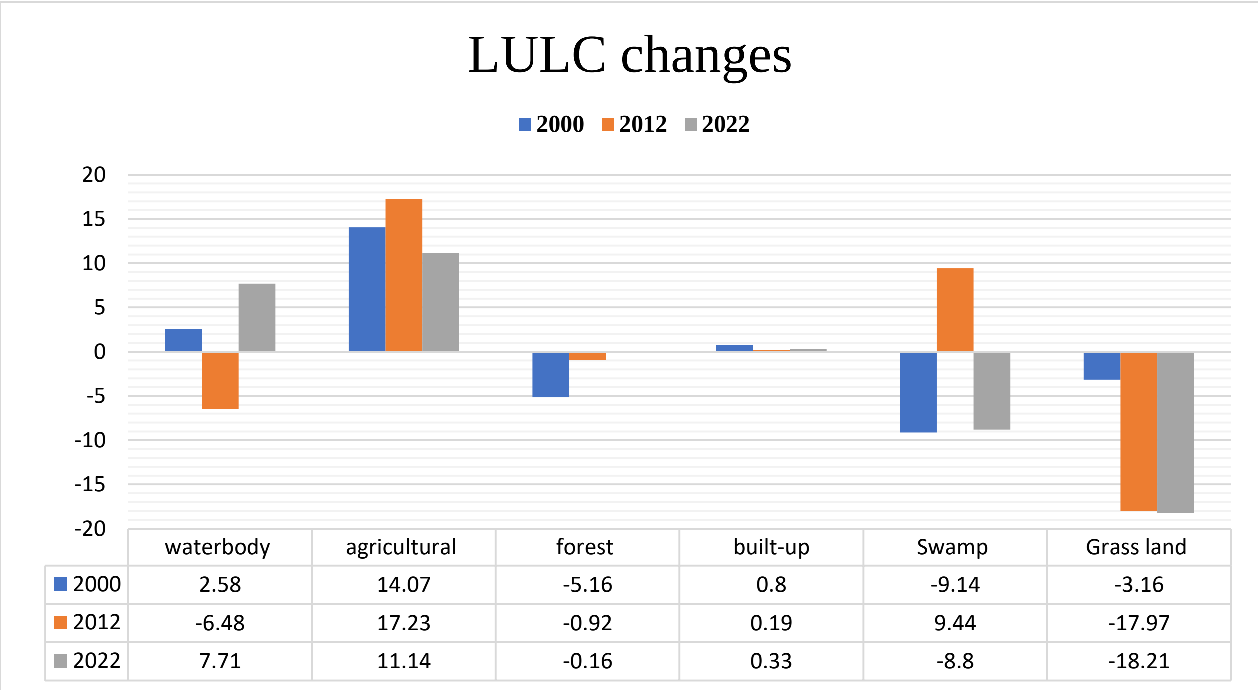

Figure 4-10 Change detection analysis

4.4.3. Impact of land use and land cover on the extent of the lake

The present study's results align with previous research that has seen comparable patterns in the decrease of Ethiopian rift valley lakes and linked these trends to both agricultural growth and land degradation (Regasa et al., 2021). These LULC changes have important ramifications for Lake Finchaa, which could affect its water quality, storage capacity, and ecological services. An investigation of satellite images from 1990 to 2022 showed significant changes in the study area land use and land cover (LULC) types. The findings showed a marked rise in the use of land for agriculture and settlement, perhaps at the expense of other land cover types such as grassland, swampland, and Finchaa Lake's water body. This pattern supports the conclusions of earlier research, which has repeatedly shown that agriculture is the main factor influencing LULC dynamics in the area (Leta et al., 2021). The water supplies in the Nile River Basin have been greatly impacted by human activity and climate change (Gedefaw et al., 2023). Additionally, the Finchaa Lake dynamic shifts in land cover and use had an effect on the water resources. Figure 4.8 shows the results of change detection for the various LULC types between 1990 and 2022. The process of rainwater runoff is greatly impacted by changes in land use and land cover. The planting of forests and the increased need for agricultural land brought about by urban development into infrastructure and settlements create a sealed surface, which has a negative impact on how precipitation is divided, leading to increased surface runoff and decreased ground water recharge (Leta et al., 2021; Moisa et al., 2023; Regasa, 2021; Sisay, 2016). Because built-up regions have a high percentage of impermeable surfaces, there is an increase in surface runoff which reduces water percolation and groundwater input to stream flow. The findings of (Goshime et al., 2019), who investigated the effects of changes in land use and land cover on the flow regimes of the lake Ziway. According to his findings, the catchment's altered land cover and use led to a decrease in base flow, an increase in runoff, a decrease in width of the river channel, and an increase in sediment deposition on the riverbank. Furthermore, the potential for Lake Finchaa to offer cultural services—which are now being explored as part of local development initiatives—may be jeopardised by the ecosystem's degradation. To summarise, the study highlights the pressing necessity of implementing efficient land use planning and management tactics to tackle the deterioration of Lake Finchaa catchment area and alleviate the detrimental effects on water resources, ecosystem services, and nearby populations. These kinds of actions are essential to maintaining the region's ecosystems, human population, and long-term sustainability of water resources. My findings indicate that while agricultural activities cause the water level of Finchaa Lake to drop, the lake's surface area increases. Result of study by Dibaba et al., (2020) show that Increased cultivation of steep slopes has increased the risk of erosion and sedimentation of nearby water bodies. Furthermore, the underlying topography of a lake is constantly changing, and elevations rise as a result of sedimentation and other human activity (Dibaba et al., 2020b).

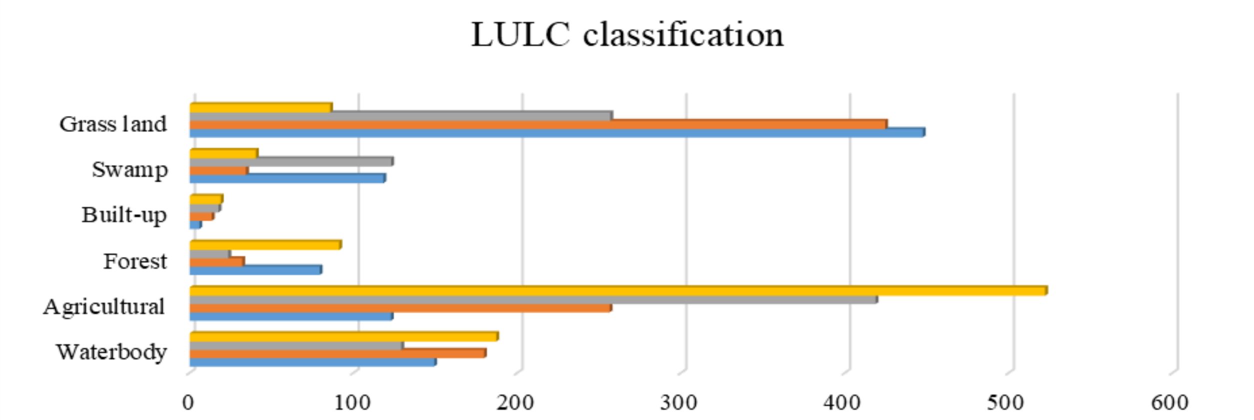

	Waterbody	Agricultural	Forest	Built-up	Swamp	Grass land
2022	187.13	522.21	91.31	19.01	40.36	85.69
2012	129.18	418.69	23.59	17.68	123.03	256.77
2000	179.64	256.39	32.09	13.47	34.38	424.54
1990	149.22	122.82	79.34	5.88	118.28	447.57

2022 2012 2000 1990

Figure 4-11 Land use patterns around the Finchaa Lake

LULC changes are dynamic and nonlinear, meaning that changes in policy, population growth, and land productivity, among other anthropogenic or natural causes, may not always result in a same pattern of conversion from one land use to another (Leta & Demissie, 2021).

4.5. Comparison of Lake area from MNDWI, AWEI and LULC

The differences in lake surface area measurements between spectral indices and Land Use/Land Cover (LULC) classification can be attributed to several factors related to methodology, data characteristics, and processing techniques. Calculating the lake surface area difference from MNDWI (Modified Normalized Difference Water Index), AWEI (Automated Water Extraction Index), and LULC (Land Use and Land Cover) involves comparing how these different methods or indices perform in identifying and quantifying water bodies

Table 4-7 surface water area of Fincha Lake between 1990 and 2022

Year	Water body area		
	MNDWI	AWEI	LULC
1990	182.13	187.84	149.22
2000	189.08	190.08	179.64
2012	173.98	176.98	129.18
2022	197.25	194.21	187.13

Spectral indices like NDWI, MNDWI, AWEI, and WRI use specific mathematical formulas that combine different spectral bands to enhance water features and suppress non-water features. These indices are sensitive to the spectral properties of water and can be affected by factors such as turbidity, vegetation, and shadows. The specific bands used and the thresholds applied can significantly impact the results. LULC classification typically involves supervised or unsupervised classification methods that categorize pixels into predefined land cover classes based on their spectral signatures. Supervised classification relies on training data that represent different land cover types. The quality and representativeness of this training data can affect the accuracy of the classification. Different classification algorithms (e.g., Maximum Likelihood, Random Forest, Support Vector Machines) have varying capabilities in distinguishing between classes, impacting the final LULC map. In generally, calculating lake surface area differences using MNDWI, AWEI, and LULC allows for a more thorough assessment of water bodies by leveraging the strengths and addressing the limitations of each method. This multi-faceted approach enhances the accuracy and reliability of water body mapping and monitoring.

4.6. Accuracy assessment of land use change

The accuracy of the entire classification is indicated by the overall accuracy, which is calculated by dividing the number of correctly classified pixels by the total number of pixels in the error matrix. The accuracy of particular classes is indicated by the other two measures. The likelihood that a pixel correctly classified on the map genuinely represents that class on the ground or reference data is considered the user's accuracy, whereas the probability that a pixel correctly classified on the reference data is considered the product's accuracy. In this study, a confusion matrix including randomly chosen points used to test accuracy using Google

Earth, land use maps, and ground truth points. Significant weight was placed on these randomly selected points' representation of various LU/LC classes.

Table 4-7 Accuracy Assessment 1990

Name of class	Waterbody	Agricultural land	Built-up	Forest land	Swamp area	Grass land	Total (User)
Waterbody	16	0	0	0	0	0	16
Agricultural land	1	37		0	1	2	41
Built-up	0	0	26	0	0	0	26
Forest land	0	0	0	17	0	0	17
Swamp area	0	0	0	1	25	1	27
Grass land	0	0	0	0	2	33	35
Total(producer)	17	37	26	18	28	34	162

$$Overall\ Accuracy = \frac{Total\ number\ of\ correctly\ \ classified\ pixels\ (Diagonal\ )}{Total\ numbr\ of\ reference\ pixels} * 100$$

$$Overall\ Accuracy = \frac{154}{162} * 100 = 95\%$$

$$UA = \frac{100 + 94 + 100 + 100 + 92 + 94}{6} = 92\%$$

$$PA = \frac{94 + 100 + 100 + 94 + 89 + 97}{6} = 96\%$$

$$Kp = \frac{(162*154) - S(16*17) + (41*37) + (26*26) + (17*18) + (27*28) + (35*34)}{162^2 - S(\ 16*17) + (\ 41*37) + (26*26) + (17*18) + (27*28) + (35*34)} * 100$$

$$Kp = \frac{24948 - 3596}{22648 - 3396} = 94\%$$

Table 4-8 Accuracy Assessment 2000

Name of class	Waterbody	Agricultural land	Built-up	Forest land	Swamp area	Grass land	Total (User)
Waterbody	11	1	0	0	0	0	12
Agricultural land	1	25	0	1	2	0	28
Built-up	0	0	13	1	1	1	16
Forest land	1	1	1	8	0	0	11
Swamp area	2	0	0	0	26	1	29
Grass land	0	0	0	1	0	15	16
Total(producer)	15	27	14	11	29	17	112

$$Overall\ Accuracy = \frac{98}{112} * 100 = 87\%$$

The average accuracy is calculated as given below:

UA= $\frac{91+89+81+72+89+89}{6} = 85\%$

The average accuracy is calculated as given below:

$$PA = \frac{73 + 92 + 93 + 73 + 88 + 90}{6} = 85\%$$

$$Kp = \frac{(112*98) - S(12*15)+(28*27)+(16*14)+(11*11)+(29*29)+(16*17)}{112^2 - S(12*15)+(28*27)+(16*14)+(11*11)+(29*29)+(16*17)}$$

$$Kp = \frac{10976-1693}{12544-1693} = 86\%$$

Table 4-9 Accuracy Assessment 2012

Name of class	Waterbody	Agricultural land	Built-up	Forest land	Swamp area	Grass land	Total (User)
Waterbody	18	0	0	0	0	0	18
Agricultural land	0	29	1	0	0	0	30
Built-up	0	1	10	0	0	1	12
Forest land	0	1	0	14	0	2	19
Swamp area	0	1	0	0	21	0	22
Grass land	0	0	0	0	2	10	12
Total(producer)	18	32	11	14	23	13	113

$$Overall\ Accuracy = \frac{102}{113} * 100 = 90\%$$

The average accuracy is calculated as given below:

$$UA = \frac{100 + 97 + 83 + 74 + 95 + 77}{6} = \mathbf{88}\%$$

The average accuracy is calculated as given below:

$$PA = \frac{100 + 90 + 91 + 100 + 91 + 91}{6} = 94\%$$

$$Kp = \frac{(113*102) - S(18*18)+(30*32)+(12*11)+(19*14)+(22*23)+(12*13)}{113^2 - S(18*18)+(30*32)+(12*11)+(19*14)+(22*23)+(12*13)}$$

$$Kp = \frac{11526-3304}{12769-3304} = 87\%$$

Table 4-10 Accuracy Assessment 2022

Name of Class	Waterbody	Agricultural land	Built-up	Forest land	Swamp area	Grass land	Total (User)
Waterbody	17	0	0	0	0	0	17
Agricultural land	0	37	1	0	1	0	39
Built-up	0	0	25	0	1		26
Forest land	0	0	0	30	0	0	32
Swamp area	0	0	0	0	20	0	20
Grass land	0	0	0	2	0	14	16
Total(producer)	17	37	26	32	22	14	150

$$Overall\ Accuracy = \frac{143}{150} * 100 = 95\%$$

The average accuracy is calculated as given below:

$$UA = \frac{100 + 95 + 96 + 94 + 91 + 87}{6} = \mathbf{94}\%$$

The average accuracy is calculated as given below:

$$PA = \frac{100 + 100 + 96 + 94 + 91 + 100}{6} = 97\%$$

$$Kp = \frac{(150 * 143) - S(17 * 17) + (39 * 37) + (26 * 26) + (32 * 32) + (20 * 22) + (16 * 14)}{150^2 - S(17 * 17) + (39 * 37) + (26 * 26) + (32 * 32) + (20 * 22) + (16 * 14)} * 100$$

$$Kp = \frac{21450 - 4096}{22500 - 4096} = 94\%$$

The accuracy of the classified maps was also assessed using the overall accuracy, producer accuracy, user accuracy, and kappa coefficient. The accuracy assessment results show an overall accuracy level of 95%, 87%, 90% and 95% for 1990, 2000, 2012 and 2022, respectively, with the corresponding Kappa statistics of 0.94, 0.86, 0.87and 0.94. The kappa coefficient ranges of all the LULCC classes were outstanding, as demonstrated by the great agreement between the classification map and the ground reference data.

The accuracy result of the land use classification is ascertained using the accuracy assessment (Islami et al., 2022). The contingency method, commonly known as the contingency matrix (confusion matrix), is the most popular technique for determining the accuracy level. The contingency matrix, according to Khalid et al., (2021), contains three types of information: kappa accuracy, overall accuracy, and producer's accuracy. The estimators of overall accuracy are the accuracy of the producer and the user. The accuracy of a map as perceived by the creator is known as the producer's accuracy, while the accuracy as seen by the user is known as the user's accuracy. Table below will provide an explanation of the accuracy test findings for the classification process. In addition, According to Basin, et al. (2020), the most popular way to represent classification accuracy is as an error matrix, from which a number of descriptive and analytical statistics can be obtained.

5. CONCLUSION AND RECOMMENDATION

5.1. CONCLUSION

The Fincha sub-basin in Ethiopia faces water scarcity, exacerbated by deforestation and agricultural expansion, which reduces reservoir capacity due to sedimentation. Despite numerous studies on global lake level changes, there is limited scientific assessment of Ethiopian lakes' surface levels, areas, and volume. The lakes surface water area was determined using the AWEI 2000 (ETM+), Modified Normalized Difference Water Index (MNDWI) for 1990 (TM), 2012 (ETM+), and 2022 (OLI_TIRS). The Fincha Lake water surface areas have shown fluctuations over the years. Accuracy indicators and estimates are provided for each water index. Overall accuracy, producer's accuracy, user's accuracy, and Kappa coefficient are all >0.83, indicating satisfactory classification accuracy. The MNDWI and AWEI exhibits the highest overall accuracy (97.5%) and kappa coefficient (0.97), demonstrating its superior ability to identify different types of water. The AWEI also demonstrates high accuracy. However, the NDWI performs less well than the MNDWI and AWEI, with lower accuracy and kappa coefficient (92.5% and 0.86, respectively). The WRI has the lowest performance among all the assessed indices, with a kappa coefficient of 0.83 and an overall accuracy of 85%. The lake water surface area declined between 2000 and 2012 before progressively increasing until 2022. The surface area of the lake was measured in January 1990, 2000, 2012, and 2022 and found to be 182.13 km^2, 190.08 km^2, 173.98 km^2, and 197.25 km^2, respectively. The largest lake area was recorded in 2022 at 197.25 km^2, while the smallest area was recorded in 2012 at 173.98 km^2. The average water surface area of Fincha Lake is approximately 185.86 km^2. The area of the lake dropped from 190.08 km^2 in 2000 to 7.95 km^2 in 2012. The lake's area has increased by 23.27 km^2 over the past 32 years. The surface area increased by around 7.95 km^2 by the year 2000. In comparison, the surface area of Fincha Lake declined by around 16.1 km^2 in 2012. In 2022, the surface area of Fincha Lake increased by 23.27 km^2. Additionally, the Finchaa Lake dynamic shifts in land cover and use had an effect on the water resources. ArcGIS software was used to determine the percentage area of each land cover class based on ML-supervised categorized images for each year independently.

5.2. RECOMMENDATION

Future studies may go deeper into the following issues, which merit particular attention. The main subjects of discussion were methods for determining lake surface area, datasets from remote sensing, and potential causes of variations.

- Research on reservoir operation and drought assessment is crucial for improving lake surface area and water use, and for detailed volume estimations for effective lake management and water scarcity issues.
- To improve validation accuracy, high-resolution data from multiple time points and cross-validation techniques should be collected to overcome challenges in sparse historical data and temporal mismatches.
- Limited ground truth data and satellite imagery may not accurately capture land cover changes in heterogeneous landscapes, necessitating the use of high-resolution satellite imagery and aerial photos for detailed analysis.

REFERENCE

Abbas, Z., & Jaber, H. S. (2020). Accuracy assessment of supervised classification methods for extraction land use maps using remote sensing and GIS techniques. *IOP Conference Series: Materials Science and Engineering*, *745*(1). https://doi.org/10.1088/1757-899X/745/1/012166

Acharya, T. D., Lee, D. H., Yang, I. T., & Lee, J. K. (2016). Identification of water bodies in a landsat 8 OLI image using a J48 decision tree. *Sensors (Switzerland)*, *16*(7), 1–16. https://doi.org/10.3390/s16071075

Acharya, T. D., Subedi, A., & Lee, D. H. (2018). Evaluation of water indices for surface water extraction in a landsat 8 scene of Nepal. *Sensors (Switzerland)*, *18*(8), 1–15. https://doi.org/10.3390/s18082580

Advisor, H. A., & Mengiste, Y. (2019). *BY: HEYRU ABDO ADVISOR: Dr. YENESEW MENGISTE OCT, 2019 ADDIS ABABA, ETHIOPIA*.

Ahmed, I. A., Shahfahad, S., Baig, M. R. I., Talukdar, S., Asgher, M. S., Usmani, T. M., Ahmed, S., & Rahman, A. (2021). Lake water volume calculation using time series LANDSAT satellite data: a geospatial analysis of Deepor Beel Lake, Guwahati. *Frontiers in Engineering and Built Environment*, *1*(1), 107–130. https://doi.org/10.1108/febe-02-2021-0009

Ali, M. I., Dirawan, G. D., Hasim, A. H., & Abidin, M. R. (2019a). *Detection of Changes in Surface Water Bodies Urban Area with NDWI and Detection of Changes in Surface Water Bodies Urban Area with NDWI and MNDWI Methods*. *June*. https://doi.org/10.18517/ijaseit.9.3.8692

Ali, M. I., Dirawan, G. D., Hasim, A. H., & Abidin, M. R. (2019b). *Detection of Changes in Surface Water Bodies Urban Area with NDWI and Detection of Changes in Surface Water Bodies Urban Area with NDWI and MNDWI Methods*. *October*. https://doi.org/10.18517/ijaseit.9.3.8692

Asfaw, W., Haile, A. T., & Rientjes, T. (2020). Combining multisource satellite data to estimate storage variation of a lake in the Rift Valley Basin, Ethiopia. *International Journal of Applied Earth Observation and Geoinformation*, *89*(March), 102095. https://doi.org/10.1016/j.jag.2020.102095

Babekir, M., & Osman, O. (2024). *The Synergy of Data Science , GIS Spatial Analysis and Knowledge Management as a Path to Sustainability Insights*. *April*, 0–18. https://doi.org/10.5772/intechopen.1002888

Basin, T. S. (2020). Land Use/Land Cover Dynamics in Upper Ribb Watershed, Lake Tana

Sub Basin, Ethiopia. *Journal of Environment and Earth Science*, 1–9. https://doi.org/10.7176/jees/10-2-01

Bulti, W. A., & Minch, A. (2019). *COMBINING SATELLITE IMAGERY AND RADAR ALTIMETRY FOR ESTIMATING LAKE ZIWAY STORAGE VARIATION*.

Buma, W. G., Lee, S. Il, & Seo, J. Y. (2018). Recent surface water extent of lake Chad from multispectral sensors and GRACE. *Sensors (Switzerland)*, *18*(7). https://doi.org/10.3390/s18072082

Chen, J., & Duan, Z. (2022). *Monitoring Spatial-Temporal Variations of Lake Level in Western China Using ICESat-1 and CryoSat-2 Satellite Altimetry*.

Cooley, S. W., Ryan, J. C., & Smith, L. C. (2021). Human alteration of global surface water storage variability. *Nature*, *591*(7848), 78–81. https://doi.org/10.1038/s41586-021-03262-3

Crétaux, J. F., Abarca-del-Río, R., Bergé-Nguyen, M., Arsen, A., Drolon, V., Clos, G., & Maisongrande, P. (2016). Lake Volume Monitoring from Space. *Surveys in Geophysics*, *37*(2), 269–305. https://doi.org/10.1007/s10712-016-9362-6

Deoli, V., Kumar, D., & Kuriqi, A. (2022). Detection of Water Spread Area Changes in Eutrophic Lake Using Landsat Data. *Sensors*, *22*(18), 1–15. https://doi.org/10.3390/s22186827

Dibaba, W. T., Demissie, T. A., & Miegel, K. (2020a). Drivers and implications of land use/land cover dynamics in Finchaa Catchment, Northwestern Ethiopia. *Land*, *9*(4), 1–22. https://doi.org/10.3390/land9040113

Dibaba, W. T., Demissie, T. A., & Miegel, K. (2020b). Watershed hydrological response to combined land use/land cover and climate change in highland ethiopia: Finchaa catchment. *Water (Switzerland)*, *12*(6). https://doi.org/10.3390/w12061801

Diress, S. A., & Besha Bedada, T. (2020). Analysis of trend of water level in case of lake tana, Ethiopia. *African Journal on Land Policy and Geospatial Sciences*, *3*(3), 2657–2664. https://doi.org/10.48346/IMIST.PRSM/ajlp-gs.v3i3.18504

Du, Y., Zhang, Y., Ling, F., Wang, Q., Li, W., & Li, X. (n.d.). *Water Bodies ' Mapping from Sentinel-2 Imagery with Modified Normalized Difference Water Index at 10-m Spatial Resolution Produced by Sharpening the SWIR Band*. https://doi.org/10.3390/rs8040354

Eghod, O. D., & Egho, L. P. E. (2016). *3HUIRUPDQFHV (YDOXDWLRQ RI 6XUIDFH : DWHU $ UHDV ([WUDFWLRQ 7HFKQLTXHV 8VLQJ / DQGVDW (70 ' DWD & DVH 6WXG \ $ VZDQ + LJK ' DP / DNH $+ '/. 22*, 1205–1212. https://doi.org/10.1016/j.protcy.2016.02.001

Experimental, A., Using, S., & Samples, R. (2023). *Modelling Spectral Unmixing of Geological Mixtures : An Experimental Study Using Rock Samples*.

Feyisa, G. L., Meilby, H., Fensholt, R., & Proud, S. R. (2014). Automated Water Extraction Index: A new technique for surface water mapping using Landsat imagery. *Remote Sensing of Environment*, *140*, 23–35. https://doi.org/10.1016/j.rse.2013.08.029

Fisher, A., Flood, N., & Danaher, T. (2016a). Comparing Landsat water index methods for automated water classification in eastern Australia. *Remote Sensing of Environment*, *175*, 167–182. https://doi.org/10.1016/j.rse.2015.12.055

Fisher, A., Flood, N., & Danaher, T. (2016b). *Remote Sensing of Environment Comparing Landsat water index methods for automated water classi fi cation in eastern Australia*. *175*, 2015–2017.

Gedefaw, M., Denghua, Y., & Girma, A. (2023). Assessing the Impacts of Land Use/Land Cover Changes on Water Resources of the Nile River Basin, Ethiopia. *Atmosphere*, *14*(4). https://doi.org/10.3390/atmos14040749

Ghansah, B., Asare, Y. M., Tchao, E. T., & Forkuo, E. K. (2016). Mapping the spatial changes in Lake Volta using multitemporal remote sensing approach. *Lakes and Reservoirs: Research and Management*, *21*(3), 206–215. https://doi.org/10.1111/lre.12138

Goshime, D. W., Absi, R., Ledésert, B., Dufour, F., & Haile, A. T. (2019). Impact of water abstraction on the water level of Lake Ziway, Ethiopia. *WIT Transactions on Ecology and the Environment*, *239*, 67–78. https://doi.org/10.2495/WS190071

Hailu, A., Mammo, S., & Kidane, M. (2020). Dynamics of land use, land cover change trend and its drivers in Jimma Geneti District, Western Ethiopia. *Land Use Policy*, *99*(October 2019), 105011. https://doi.org/10.1016/j.landusepol.2020.105011

Hailu, B. T., & Girma, S. (2019). *Spatio Temporal Lake Level Change of Lake Abijata , Ethiopia : A Remote Spatio Temporal Lake Level Change of Lake Abijata , Ethiopia : A Remote Sensing Approach*. *July*. https://doi.org/10.31031/EAES.2019.06.000627

Huang, C., Chen, Y., Zhang, S., & Wu, J. (2018). Detecting, Extracting, and Monitoring Surface Water From Space Using Optical Sensors: A Review. *Reviews of Geophysics*, *56*(2), 333–360. https://doi.org/10.1029/2018RG000598

Ibrahim, M. M., & Al-fugara, A. K. (2022). *CO*. *January*. https://doi.org/10.30955/gnj.004018

Islam, M. S., & Mostafa, M. G. (2024). Impacts of Climate Change on Global Freshwater Quality and Availability: A Comprehensive Review. *Journal of Water and Environment*

Technology, *22*(1), 1–26. https://doi.org/10.2965/jwet.23-036

Islami, F. A., Tarigan, S. D., Wahjunie, E. D., & Dasanto, B. D. (2022). Accuracy Assessment of Land Use Change Analysis Using Google Earth in Sadar Watershed Mojokerto Regency. *IOP Conference Series: Earth and Environmental Science*, *950*(1). https://doi.org/10.1088/1755-1315/950/1/012091

Ismail, M. A., Waqas, M., Ali, A., Muzzamil, M. M., Abid, U., & Zia, T. (2022). Enhanced index for water body delineation and area calculation using Google Earth Engine: a case study of the Manchar Lake. *Journal of Water and Climate Change*, *13*(2), 557–573. https://doi.org/10.2166/wcc.2021.282

Jeihouni, M., Toomanian, A., Alavipanah, S. K., & Hamzeh, S. (2017). Quantitative assessment of Urmia Lake water using spaceborne multisensor data and 3D modeling. *Environmental Monitoring and Assessment*, *189*(11). https://doi.org/10.1007/s10661-017-6308-5

Ji, R. P., Yu, W. Y., Feng, R., Wu, J. W., & Zhang, Y. S. (2019). The threshold determination methods of water body information extraction using GF-1 satellite image. *IOP Conference Series: Materials Science and Engineering*, *592*(1). https://doi.org/10.1088/1757-899X/592/1/012088

Kabite, G., Muleta, M. K., & Gessesse, B. (2020). Spatiotemporal land cover dynamics and drivers for Dhidhessa River Basin (DRB), Ethiopia. *Modeling Earth Systems and Environment*, *6*(2), 1089–1103. https://doi.org/10.1007/s40808-020-00743-8

Karpatne, A., Khandelwal, A., Chen, X., Mithal, V., Faghmous, J., & Kumar, V. (2016). Global monitoring of inland water dynamics: State-of-the-art, challenges, and opportunities. *Studies in Computational Intelligence*, *645*, 121–147. https://doi.org/10.1007/978-3-319-31858-5_7

Kenea, U., Adeba, D., Regasa, M. S., & Nones, M. (2021). Hydrological responses to land use land cover changes in the fincha'a watershed, Ethiopia. *Land*, *10*(9). https://doi.org/10.3390/land10090916

Khalid, H. W., Khalil, R. M. Z., & Qureshi, M. A. (2021). Evaluating spectral indices for water bodies extraction in western Tibetan Plateau. *Egyptian Journal of Remote Sensing and Space Science*, *24*(3), 619–634. https://doi.org/10.1016/j.ejrs.2021.09.003

Kushwaha, N. L., Elbeltagi, A., Patel, A., Zakwan, M., Rajput, J., & Sharma, P. (2022). *Assessment of water resources using remote sensing and GIS techniques*. *October*, 85–98. https://doi.org/10.1016/b978-0-323-91910-4.00006-6

Lemi, T. (2019). *Threats and Opportunities of Central Ethiopia Rift Valley Lakes*. *22*(2).

https://doi.org/10.19080/IJESNR.2019.22.556082

Leta, M. K., & Demissie, T. A. (2021). Modeling and prediction of land use land cover change dynamics based on land خوب. *Sustainability (Switzerland)*, *13*(7).

Leta, M. K., Demissie, T. A., & Tränckner, J. (2021). Hydrological Responses of Watershed to Historical and. *Water (Switzerland)*, *13*(17).

Li, X., Zhang, F., Chan, N. W., Shi, J., Liu, C., & Chen, D. (2022). High Precision Extraction of Surface Water from Complex Terrain in Bosten Lake Basin Based on Water Index and Slope Mask Data. *Water (Switzerland)*, *14*(18). https://doi.org/10.3390/w14182809

Lin, Y., Li, X., Zhang, T., Chao, N., Yu, J., Cai, J., & Sneeuw, N. (2020). Water volume variations estimation and analysis using multisource satellite data: A case study of Lake Victoria. *Remote Sensing*, *12*(18). https://doi.org/10.3390/RS12183052

M, K. K., Bd, P., Prabu, S., & Ullo, S. (2020). *Comparative Analysis to Identify Efficient Technique for Interfacing BCI System Comparative Analysis to Identify Efficient Technique for Interfacing BCI System*. https://doi.org/10.1088/1757-899X/925/1/012062

Mcfeeters, S. K. (2007). *The use of the Normalized Difference Water Index (NDWI) in the delineation of open water features*. *1161*. https://doi.org/10.1080/01431169608948714

Minale, A. S. (2020a). Water level fluctuations of Lake Tana and its implication on local communities livelihood, northwestern Ethiopia. *International Journal of River Basin Management*, *18*(4), 503–510. https://doi.org/10.1080/15715124.2019.1700512

Minale, A. S. (2020b). Water level fluctuations of Lake Tana and its implication on local communities livelihood, northwestern Ethiopia. *International Journal of River Basin Management*, *18*(4), 503–510. https://doi.org/10.1080/15715124.2019.1700512

Modeling, H., Analysis, W., Swat, O. F., Basin, R., Using, B. Y., Model, H. B. V. L., & Gis, A. R. C. (2023). *HYDROLOGICAL MODELING AND WATERSHED ANALYSIS OF SWAT RIVER BASIN BY USING*.

Mohammed, J. I. (2020). Application of HEC-HMS for the Assessment of Water Availability in Fincha and Didessa Sub-basin, Ethiopia. *Journal of Environment and Earth Science*, *10*(11). https://doi.org/10.7176/jees/10-11-05

Moisa, M. B., Hinkosa, L. B., Negasa, G. F., Olika, G., Ijigu, T. E., Wedajo, Y. N., Gurmessa, M. M., Deribew, K. T., & Gemeda, D. O. (2023). GIS and remote sensing Based Analysis of Land use and Land cover Change in the Upper Anger watershed , Western Ethiopia. *Geology, Ecology, and Landscapes*, *00*(00), 1–10. https://doi.org/10.1080/24749508.2023.2237323

Muralitharan, J., Gunalan, J., Duraisamy, R., & Ersulo, A. A. (2021). *Study the Relationship*

Between LULC , LST , NDVI , NDWI and NDBI in Greater Arba Minch Area , Rift. *September*. https://doi.org/10.2991/ahis.k.210913.023

Naik, B. C., & Anuradha, B. (2020). *Extraction of Spread Surface Water Body using Supervised and Unsupervised Classification Techniques*. *3878*(6), 2345–2350. https://doi.org/10.35940/ijrte.F8421.038620

Nandi, D., Chowdhury, R., Mohapatra, J., Mohanta, K., & Ray, D. (2018). Automatic Delineation of Water Bodies Using Multiple Spectral Indices. *International Journal of Scientific Research in Science, Engineering and Technology*, *4*(4), 498–512.

Pekel, J. F., Cottam, A., Gorelick, N., & Belward, A. S. (2016). High-resolution mapping of global surface water and its long-term changes. *Nature*, *540*(7633), 418–422. https://doi.org/10.1038/nature20584

Regasa, M. S. (2021). *Historical and future land use and land cover changes in the Fincha watershed , Ethiopia*. 1–19.

Regasa, M. S., & Nones, M. (2022a). *Land Use Land Cover Changes in the Fincha Basin, Ethiopia*. *June*, 840–844. https://doi.org/10.3850/iahr-39wc252171192022689

Regasa, M. S., & Nones, M. (2022b). *Land Use Land Cover Changes in the Fincha Basin , Ethiopia Land Use Land Cover Changes in the Fincha Basin , Ethiopia*. *June*. https://doi.org/10.3850/IAHR-39WC252171192022689

Regasa, M. S., Nones, M., & Adeba, D. (2021). A review on land use and land cover change in ethiopian basins. *Land*, *10*(6), 1–13. https://doi.org/10.3390/land10060585

Region, L. (2020). *on FengYun Satellite Data : A Case Study of Poyang*.

Sathianarayanan, M. (2018). *ASSESSMENT OF SURFACE WATER DYNAMICS USING MULTIPLE WATER INDICES AROUND ADAMA WOREDA , ETHIOPIA*. *IV*(November), 20–23.

Shen, L., & Li, C. (2010). Water body extraction from Landsat ETM+ imagery using adaboost algorithm. *2010 18th International Conference on Geoinformatics, Geoinformatics 2010*, *2008*, 3–6. https://doi.org/10.1109/GEOINFORMATICS.2010.5567762

Shift, R., Lake, T., & Ziway, L. (2021). *Satellite Imageries and Field Data of Macrophytes Reveal a*.

Shumet, A. G., & Mengistu, K. T. (2016). *Geosciences and Geophysics*. *5*(5), 8719.

Sisay, A. (2016). Remote Sensing Based Water Surface Extraction and Change Detection in the Central Rift Valley Region of Ethiopia. *American Journal of Geographic Information System*, *5*(2), 33–39. https://doi.org/10.5923/j.ajgis.20160502.01

Sun, Q., & Li, J. (2024). OPEN A method for extracting small water bodies based on DEM and remote sensing images. *Scientific Reports*, *0123456789*, 1–11. https://doi.org/10.1038/s41598-024-51346-7

Tesfaye, M., & Breuer, L. (2023). *Performance of water indices for water resources monitoring using large-scale Sentinel-2 data*. *May*, 1–11. https://doi.org/10.20944/preprints202305.2125.v1

Tewabe, D., & Fentahun, T. (2020). Assessing land use and land cover change detection using remote sensing in the Lake Tana Basin, Northwest Ethiopia. *Cogent Environmental Science*, *6*(1). https://doi.org/10.1080/23311843.2020.1778998

Treichler, D., Kääb, A., Salzmann, N., & Xu, C. Y. (2019). Recent glacier and lake changes in High Mountain Asia and their relation to precipitation changes. *Cryosphere*, *13*(11), 2977–3005. https://doi.org/10.5194/tc-13-2977-2019

Wang, Rui, Guo, L., Chen, B., Yang, Y., Zheng, H., Deng, F., & Liu, J. (2023). Spatiotemporal variations and overflow risk analysis of the Salt Lake in the Hoh Xil Region using machine learning methods. *Frontiers in Earth Science*, *10*(January), 1–14. https://doi.org/10.3389/feart.2022.1084540

Wang, Ruimeng, Pan, L., Niu, W., Li, R., Zhao, X., Bian, X., Yu, C., Xia, H., & Chen, T. (2021). Monitoring the spatiotemporal dynamics of surface water body of the Xiaolangdi Reservoir using Landsat-5/7/8 imagery and Google Earth Engine. *Open Geosciences*, *13*(1), 1290–1302. https://doi.org/10.1515/geo-2020-0305

Water, L. S., Analysis, D., & Basin, R. (2018). *Long-Term Surface Water Dynamics Analysis Based on Landsat Imagery and the Google Earth Engine Platform : A Case Study in the Middle Yangtze River Basin*. https://doi.org/10.3390/rs10101635

Wu, Q., Yue, H., Liu, Y., & Hou, E. (2021a). Geospatial quantitative analysis of the Aral Sea Shoreline changes using RS and GIS techniques. *Earth Science Informatics*, *October*. https://doi.org/10.1007/s12145-021-00714-2

Wu, Q., Yue, H., Liu, Y., & Hou, E. (2021b). Geospatial quantitative analysis of the Aral Sea Shoreline changes using RS and GIS techniques Geospatial quantitative analysis of the Aral Sea Shoreline changes using RS and GIS techniques. *Earth Science Informatics*, *October*. https://doi.org/10.1007/s12145-021-00714-2

Xu, H. (2006). Modification of normalised difference water index (NDWI) to enhance open water features in remotely sensed imagery. *International Journal of Remote Sensing*, *27*(14), 3025–3033. https://doi.org/10.1080/01431160600589179

Xu, H. (2019). *Modification of Normalized Difference Water Index (NDWI) to Enhance*

Open Water Features in Remotely Sensed Imagery. *March*. https://doi.org/10.1080/01431160600589179

Ye, Z., Liu, H., Chen, Y., Shu, S., Wu, Q., & Wang, S. (2017). Analysis of water level variation of lakes and reservoirs in Xinjiang, China using ICESat laser altimetry data (2003–2009). *PLoS ONE*, *12*(9), 1–21. https://doi.org/10.1371/journal.pone.0183800

Yulianto, F., Kushardono, D., Budhiman, S., Nugroho, G., Chulafak, G. A., Dewi, E. K., & Pambudi, A. I. (2022). Evaluation of the Threshold for an Improved Surface Water Extraction Index Using Optical Remote Sensing Data. *Scientific World Journal*, *2022*. https://doi.org/10.1155/2022/4894929

Zhang, F. F., Zhang, B., Li, J. S., Shen, Q., Wu, Y., & Song, Y. (2011). Comparative analysis of automatic water identification method based on multispectral remote sensing. *Procedia Environmental Sciences*, *11*(PART C), 1482–1487. https://doi.org/10.1016/j.proenv.2011.12.223

Zhang, F., Li, J., Zhang, B., Shen, Q., Ye, H., Wang, S., & Lu, Z. (2018). A simple automated dynamic threshold extraction method for the classification of large water bodies from landsat-8 OLI water index images. *International Journal of Remote Sensing*, *39*(11), 3429–3451. https://doi.org/10.1080/01431161.2018.1444292

Zhang, Y., Liu, X., Zhang, Y., Ling, X., & Huang, X. (2018). Automatic and Unsupervised Water Body Extraction Based on Spectral-Spatial Features Using GF-1 Satellite Imagery. *IEEE Geoscience and Remote Sensing Letters*, *PP*, 1–5. https://doi.org/10.1109/LGRS.2018.2886422